EFFECT OF SLAG COMPOSITION AND MORPHOLOGY ON PHOSPHOROUS DISTRIBUTION IN STEEL MAKING

A Thesis submitted
In Partial Fulfillment of the Requirements
For the Degree of
MASTER OF TECHNOLOGY

BY
JAYANTA HALDER
(Y110607)

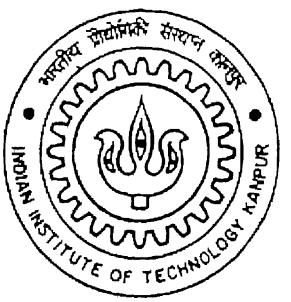

To the
Department of Materials & Metallurgical Engineering
Indian Institute of Technology, Kanpur
July, 2003

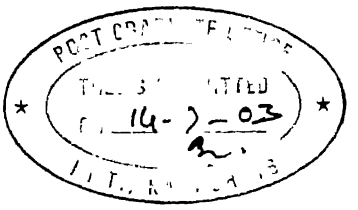

Certificate

This is to certify that the work contained in this thesis entitled *"Effect of slag composition and morphology on phosphorous distribution in steel making"* by Mr Jayanta Halder (Roll No. Y110607) has been carried out under my supervision and this work has not been submitted elsewhere for the award of a degree.

July 2003

Dr. Brahma. Deo
Professor
Department of Materials and Metallurgical Engineering
I.I T., Kanpur

Dedicated to
My Parents

ACKNOWLEDGEMENT

First of all, I am grateful to Professor Brahma Deo for guiding me in my first venture in engineering research. Our technical and non-technical discussions kept the spirits high, thus, making the stay at I.I.T., Kanpur motivating and enjoyable. Moreover his guidance has helped me to develop the various facets of my personality.

Words are insufficient to describe my indebtness to my parents whose encouragement and guidance have helped me strive forward throughout the Masters program.

I wish to thank my friends, specially Debu, Pramod, Somnath Basu, Sonada, Gmon, Natida, Saubhik, Avishekh, Debraj. Their company made my stay at I.I.T., Kanpur enjoyable.

Table of contents

List of Tables

List of Figures

List of Symbols

(Al_2O_3)	Percent (Al_2O_3) in slag at tap
C_2	Mass percent carbon in metal at the end of the blow.
C_2S	Dicalcium-silicate
(CaO)	Percent CaO in slag at tap
$Dolo_2$	Dolomite added during the 2^{nd} part of the blow
(FeO)	Percent FeO in slag at tap
HL_2	Lance height during 2^{nd} part of blow, cm
HTR	Hot metal to scrap ratio
Mn_2	Mass percent manganese in metal at the end of the blow.
(MnO)	Percent MnO in slag at tap
(MgO)	Percent MgO in slag at tap
Ore	Total amount of ore added.
Ore_2	Ore added during 2^{nd} part of the blow
P_2	Mass percent phosphorous in metal at the end of the blow
(P_2O_5)	Percent P_2O_5 in slag at tap
R	Correlation coefficient
$Rdolo_2$	Raw dolomite added during 2^{nd} part of the blow
(SiO_2)	Percent SiO_2 at tap
SVO	Slag mass at tap
T_2	Tapping temperature of metal
σ	Standard deviation
$\wedge$	Optical basicity

Abstract

The models available for prediction of phosphorus in steel are reviewed. Healy's model molecular slag model, optical basicity model and quadratic formalism model are selected and tuned and tested for the data collected from different plants. In order to improve the prediction, additional parameters like ore added, lance height, end point carbon content, etc., are included in the models. The effect of different starting conditions of phosphorous (0.06-0.26P) and Si (0.3-1.2 Si) in hot metal and also the composition of slag, MgO (0.5-11%), Al_2O_3 (0.5-4%), FeO (12-25%), have been examined under SEM and optical microscope to find out the effects of MgO and Al_2O_3 on slag morphology and distribution of the phosphorous in different phases. It is observed that molecular slag model gives best results for prediction of phosphorous at tap. Distribution of phosphorous in di-calcium silicate and in wustite solid solution or in the liquid slag is examined assuming different ratios of P_2O_5 in di-calcium silicate and in liquid slag. The prediction improves marginally when percent di-calcium silicate is also included as a parameter in the molecular slag model.

Chapter-1

Introduction

Production of low phosphorous steel containing less than 0.015% phosphorous in a single blow in the BOF, when the phosphorous content in hot metal is high (above 0.2%) and silicon content is variable (0.6-1.2% Si) is a challenging problem. Even though a pseudo steady state is usually attained between slag and metal towards the end of the blow, it is difficult to estimate the distribution of phosphorous by application of thermodynamics alone. This is partly due to the lack of free energy and activity data in multi component, multiphase slag systems with many components such as P_2O_5, FeO, MgO, CaF_2, SiO_2, and CaO. Phosphorous distribution also depends upon variations in operating parameters, such as slag mass, turndown carbon, basicity of slag, and initial phosphorous content of metal, intensity of bottom stirring, lance height, oxygen flow rate addition scheme and time of addition of fluxes.

In recent times, a high percentage of continuous casting has posed additional problems due to centre line segregation of phosphorous, which causes hydrogen-induced cracking and heat affected zone cracking during welding. Further, the molten steel for continuous casting is tapped at a higher temperature, and the chances of reversion of phosphorous at the end of the blow is high

In the present work, several models reported in literature have been tested and then improved using stepwise multiple linear regression. The models published so far did not take into account the effect of precipitation and dissolution of dicalcium silicate (C_2S) on phosphorous distribution. It is now well established that C_2S has higher solubility for phosphorous than the liquid part of slag, which is mainly wustite solid solution.

The fraction of dicalcium silicate is also calculated from ternary phase diagram considering that slag is quasi-ternary ($CaO-FeO-SiO_2$). This calculated fraction of C_2S is also incorporated as a parameter into regression analysis. The activity of FeO needed for calculation of phosphorous distribution is calculated by different methods and incorporated as a parameter into regression in the case of quadratic formalism model. In this work effort has been made to evolve a strategy to find the best possible method of phosphorous prediction for a given shop floor situation by analyzing actual plant data from different steel plants. The focus is to study the effect of MgO and Al_2O_3 in phosphorous distribution. This is supplemented by morphological investigations (optical, SEM, EPMA and X-RD).

Chapter-2

Models for prediction phosphorous distribution

2.0 Introduction:

Several models have been reported in literature, for a particular plant situation, it is desired to choose a model which gives best results for the given plant condition. Various models for prediction phosphorus distribution are reviewed in this chapter.

2.1 Balajiva's model

Balajiva et al [1] proposed a model for prediction of phosphorous partition is as follows;

$$\log\frac{(P)}{[P]} = 5.9\times\log(CaO) + 2.5\times\log(FeO) + 0.5\times\log(P_2O_5) + 10.6 \qquad \ldots\ldots\ldots\ldots (2.1)$$

In the above model turndown temperature is not taken as a parameter. According to this model phosphorus partition essentially depends upon mass percent CaO, mass percent FeO and mass percent P_2O_5 in slag.

2.2 Turkdogan's model

Turkdogan[2] developed a correlation from plant data is as follows;

$$\log\frac{(P)}{[P]\times[O]^{2.5}} = \frac{27140}{T} - 9.87 + 0.071[(CaO) + (CaF_2) + 0.3(MgO)] \qquad \ldots\ldots\ldots\ldots\ldots\ldots (2.2)$$

Where, [O] is mass percent oxygen in metal.

(CaO) is mass percent CaO in slag.

(MgO) is mass percent MgO in slag.

(CaF_2) is mass percent (CaF_2) in slag.

In the above model effect of MgO and CaF_2 on phosphorous distribution is included as a parameter.

2.4 Healy's model [3] based on ionic theory of slag:

Healy's model is essentially based on ionic theory of slag. The following equation was developed from thermodynamic data on phosphorous activity and phosphate free energy.

$$\log\frac{(P)}{[P]} = \frac{22350}{T} + 0.08\times(CaO) + 2.5\times\log(Fe_t) - 16 \qquad \ldots\ldots\ldots\ldots (2.3)$$

Where (P) is mass % of phosphorus in slag

[P] Mass % of phosphorus in metal

Fe_t is mass % of Fe in slag, calculated from total amount of different iron oxides present in the slag.

(CaO) is mass % of CaO in slag.

T is turndown temperature in Kelvin.

Healy's equation gives good estimate of the distribution of phosphorous between molten iron and complex slag of the CaO-FeO_t-SiO_2 system containing normal amounts of MgO, MnO, and Al2O3.

According to equation 2.3, phosphorous partition depends on three parameters temperature (T), mass % of Fe in slag, mass % of CaO in slag.

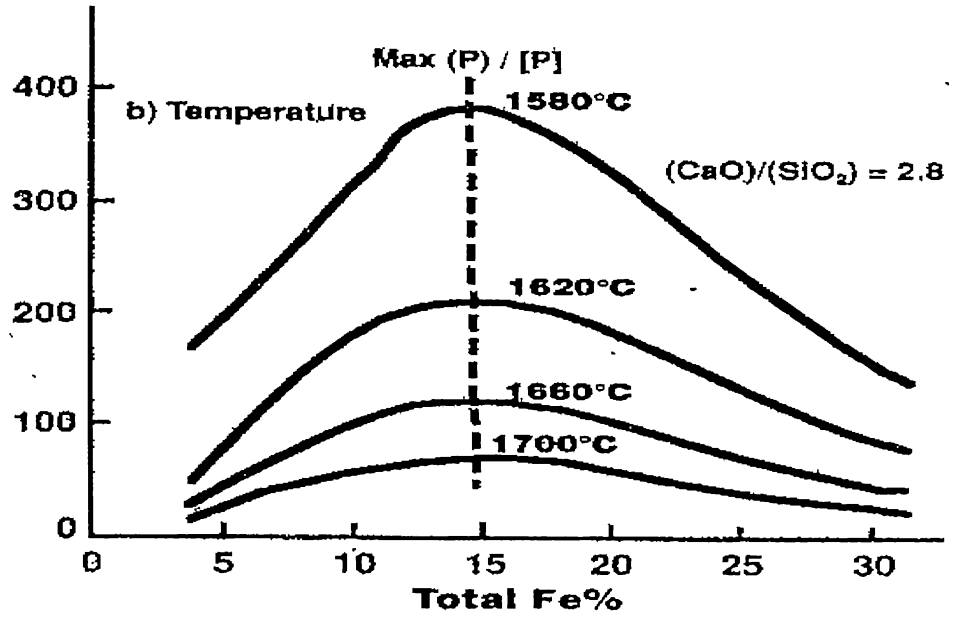

Fig-2.1 The effect of (FeO) and turn down temperature on phosphorous partition coefficient [4]

The effect of FeO and temperature (at a fixed basicity of 2.8)on phosphorous distribution is shown in Fig 2.1. It is clear that at the beginning the phosphorous partition increases with increasing FeO and reaches maxima (at around 15-20% (FeO). Beyond 20% (FeO) phosphorous distribution ratio decreases, this is because for a given mass of slag, higher FeO means low CaO. Thus, there exists an optimum FeO content for a given basicity. Higher the temperature, lower is the phosphorous distribution. The combined effect of FeO and basicity is shown in Fig 2.2. It can be seen that phosphorous distribution improves as basicity increases but the maxima shifts gradually towards left as basicity increases.

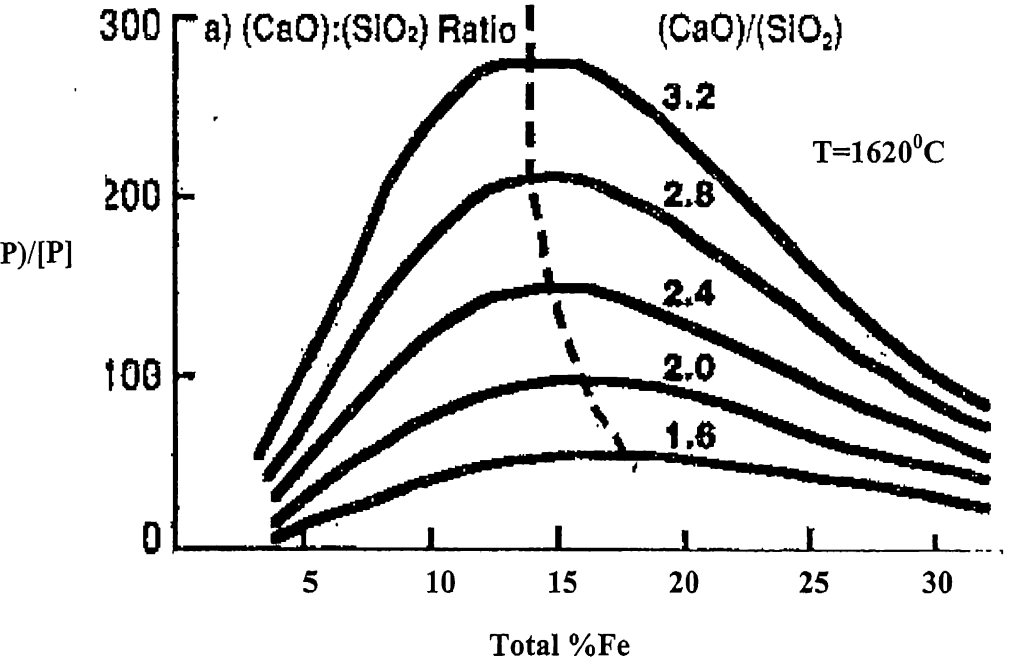

Fig-2.2 Combined effect of basicity and (FeO) on dephosphorisation [4]

2.5 Optical basicity model

According to optical basicity [5] model the phosphorus distribution is given by,

$$\log\frac{(\%p)}{[\%p]} = 16.7825\Lambda + \frac{17899.5}{T} - 18.975 \quad \text{.....} \quad \text{.....} \quad \text{.....} \quad \text{.....} \quad \text{...(2.4)}$$

The optical basicity, Λ, for a complex slag is calculated as,

$$\Lambda = \Lambda_1 X_1 + \Lambda_2 X_2 + \ldots \quad \text{.....} \quad \text{.....} \quad \text{.....} \quad \text{..(2.5)}$$

Where,

X_i is equivalent fraction component oxides
Λ_i is optical basicity of component oxides.

Optical basicity can be calculated from

$$\Lambda = \frac{\sum \frac{W_i O_i \Lambda_i}{M_i}}{\sum \frac{W_i O_i}{M_i}} \quad \text{..... (2.6)}$$

Where,
W_i is mass % of species.
O_i number of oxygen atoms in the molecule.
M refer to molecular mass
O_i/M_i is called oxidation number coefficient (known also as O/M ratio, for example O/M ratio for CaO is 2/56=0.375 where 2 is charge of cation Ca^{2+} and 56 is the molecular mass of CaO).

An improvement of equation (2.6), has been suggested [6]

$$\log C_P = -18184 + 35.84 \times \Lambda - 22.35 \times \Lambda^2 + 22930 \times \frac{\Lambda}{T} - 0.06257 \times FeO$$
$$-0.04256 \times MnO + 0.359 \times P_2O_5^{0.3} \quad \text{.....(2.7)}$$

In this equation the parameters which have been included are optical basicity, temperature, FeO, MnO, and P_2O_5. The use of P_2O_5 on right hand side of the above equation probably reflects the need for self-interacting coefficient for some components.

2.6 Suito's model

Suito developed the following relationship for the phosphorous distribution;

$$\log \frac{(P)}{[P] \times (Fe_t)^{\frac{5}{2}}} = 0.720 \times [(CaO) + 0.3 \times (MgO) +).6 \times P_2O_5 + 0.6 \times (MnO)]$$
$$+ \frac{11570}{T} - 10.520 \quad \text{.....(2.8)}$$

Where,

(Fe_t) total mass percent of Fe in slag

The above correlation includes the effect of MgO and MnO on phosphorous partition.

2.7 Suito and Inoue's model

Suito and Inoue[7] reported that the phosphorous distribution data can be correlated by the expression;

$$\log(K_P) = 0.145\times[(CaO)+0.3\times(MgO)+0.6\times(MnO)]+\frac{22810}{T}-20.506 \quad \text{.....(2.9)}$$

According to equation (2.9) the phosphorous partition depends upon mass percent CaO, mass percent of MgO, pass percent of P_2O_5, mass percent of MnO in slag, and turndown temperature.

Where K_P is $K_p = \dfrac{a_{P_2O_5}}{[h_p]^2(h_O)^5}$

(CaO) is mass percent CaO in slag.

(MgO) is mass percent MgO in slag.

(MnO) is mass percent MnO in slag.

(P_2O_5) is mass percent P_2O_5 in slag.

2.8 Elliott's model

A correlation was proposed by Elliott et al [8]. Considering the phosphorous reaction:

$$\frac{1}{2}P_2(g)+\frac{5}{4}O_2(g)+\frac{3}{2}(O^{2-}) = (PO_4^{3-}) \quad \text{..... ...(2.10)}$$

The equilibrium constant for reaction (2.10) is given by the expression:

$$\ln \frac{N_{PO_4^{3-}}\gamma_{PO_4^{3-}}}{P_{P_2}^{1/2}P_{O_2}^{5/4}N_{2-}^{3/2}\gamma_{O_{2-}}^{3/2}} = \sum_i N'_{C_i} \ln K_i \quad \text{.....(2.11)}$$

Where $N_{PO_4^{3-}}$ and $N_{O_{2-}}$ are the anionic mole fractions of phosphate and oxygen ions, N'_{C_i} is an electrical equivalent cationic mole fraction, γ_i is activity coefficient, and K_i is the equilibrium constant for exchange reaction, e.g., for calcium:

$$\frac{1}{2}P_2(g)+\frac{5}{4}O_2(g)+\frac{3}{2}CaO(l) = \frac{1}{2}Ca_3(PO_4)_2(l) \quad \text{.....(2.12)}$$

The basic slag is presumed to consist of only the cations Ca^{2+} Mg2+, Mn2+, and the anions AlO3-, FeO_3^{3-} $P_3^{3-}, SiO_4^{4-}, S^{2-}, F^-, O^{2-}$

2.9 Molecular slag model

According to molecular slag model
$2P + 5FeO = P_2O_5 + 5Fe$

%Fe in slag is calculated from total amount of iron oxide present in the slag

$$\log \frac{(\%P2O5)}{[\%p]^2\ (\%Fe)^5} = 7.04 \log(\%CaO) + \frac{9922}{T_c + 17.78} - 20.2 \quad \text{.....(2.13)}$$

where T_c is temperature in centigrade,
[%p] is mass % of phosphorus in metal,
($\%P_2O_5$) is mass % P_2O_5 in slag,
(%Fe) is mass % of Fe in slag, and
(%CaO) is mass % of CaO in slag;

The constants 7.041, 9922, 17.78 may vary, depending upon the situation at a particular plant.

2.10 Quadratic formalism model

Quadratic formalism model was proposed by Ban Ya et al [9]. It is based on regular solution model to calculate the interaction parameters between slag components. According to this model the basic reaction for oxidation of phosphorus is considered as $2[P] + 5[O] = (P_2O_5)$.

The activity of P_2O_5 in a regular solution (expressed as $aPO_{2.5}$) is given by

$$RT \ln a_{P2O5}(l) = RT \ln a_{P2O5(RS)} + 52720 - 230.706T$$

$$= 2RT \ln \gamma_{PO2.5(RS)} + 2RT \ln X_{PO2.5}(RS) + 52720 - 230.706T \quad \text{.....(2.14)}$$

Where RS stands for regular solution.

In a slag (containing CaO, FeO, MgO, MnO, etc.) the mole fraction of $PO_{2.5}$ is calculated as

$$X_{PO2.5} = \frac{\frac{m_{P2O5}}{M_{PO2.5}}}{\frac{m_{P2O5}}{M_{PO2.5}} + \frac{m_{CaO}}{M_{CaO}} + \frac{m_{SiO2}}{M_{SiO2}} + \frac{m_{MgO}}{M_{MgO}} + \frac{m_{MnO}}{M_{MnO}} + \frac{m_{FeO}}{M_{FeO}}} \quad \text{----------(2.15)}$$

Where m_i is mass of oxide and M_i is the corresponding molecular mass. According to quadratic formalism, the activity coefficient of $PO_{2.5}$, expressed as $\gamma_{PO2.5}$, can be calculated in terms of interaction parameters between binary components, say CaO, FeO, SiO_2, and MgO by using the equation,

$$RT\ln\gamma_{PO2.5(RS)} = -251040X_{CaO}^2 + 83680X_{SiO2}^2 - 37660X_{MgO}^2 - 84940X_{MnO}^2 - 31380X_{FeO}^2 - 33470X_{CaO}X_{SiO2} - 188280X_{CaO}X_{MgO} - 243930X_{CaO}X_{MnO} - 251040X_{CaO}X_{FeO} + 112960X_{SiO2}X_{MgO} + 74050X_{SiO2}X_{MnO} + 94140X_{SiO2}X_{FeO} - 184520X_{MgO}X_{MnO} - 102510X_{MgO}X_{FeO} - 123430X_{MnO}X_{FeO} \quad \text{.....(2.16)}$$

Now, for the reaction 2[P] + 5[O] = (P_2O_5), the equilibrium constant is

$$K_p = \frac{a_{P_2O_5}}{[h_p]^2(h_o)^5} \quad \text{.....(2.17)}$$

And,

$$-RT\ln K_P = -705420 + 556.472 \times T \quad \text{.....(2.18)}$$

$$RT\ln[\%P] = RT\ln aP_2O_5 - 5RT\ln[\%O] - RT\ln K_P \quad \text{.....(2.19)}$$

For known values of $\ln(a_{P_2O_5})$, ln [%O], and lnKp at a given temperature, [%P] can be calculated from (Eq2.19). The value of oxygen in metal is calculated by estimating the activity of FeO in slag. Three different methods are used to calculate activity of FeO in slag, hence the oxygen content of metal are explained in Appendix-A. But all the methods give almost same correlation coefficient. Therefore only regular solution method is followed for the calculation of activity of FeO.

Chapter-3

Experimental data collected from steel plant

3.0 Introduction

The details of data collected from steel plants for four different case studies are presented here. The plant data for case study-1 pertains to low phosphorous (<0.07%P) hot metal and low MgO (<2%MgO) slag practice. The plant data for case study-2 is for high initial phosphorous (0.2-0.26%P) hot metal and low MgO (<2%MgO) slag practice. The plant data for case study 3 is for low initial phosphorous (<0.07%) hot metal and high MgO slag (7-11% MgO) practice. In the case study-4, data from 3 more plants is collected to study the effect of MgO and Al_2O_3 on slag morphology at tap and the distribution of phosphorous in different phases, including the precipitation and also dissolution of dicalcium silicate.

3.1 Data for case study-1: (low initial phosphorous and low MgO in slag)

In case study-1, for a 300 ton BOF with bottom stirring, sub-lance is used for in blow measurements. The data is collected for 400 heats and then regrouped on the basis of additions of ore during the 2^{nd} part of blow (Ore_2) and raw dolomite during 2^{nd} part of the blow ($Rdolo_2$). The data set-1 contains heats in which no raw dolomite is added during 2^{nd} part of the blow but ore has been added during 2^{nd} part of the blow The data set-2 contains heats in which neither ore nor raw dolomite has been added during the 2^{nd} part of the blow. Data set-3 contain heats in which raw dolomite has been added but ore has not been added during the 2^{nd} part of the blow. The details of data sets (with minimum and maximum of each parameter) are given in the Table 3.1.

3.2 Data for case study-2: (high initial phosphorous and low MgO in slag)

In case study-2, for a 140 ton BOF with bottom stirring, data of approximately 400 heats has been analyzed for the three separate converters (vessel 1, 2 and 3). Filtering is done to eliminate bad/abnormal data, or data which violate the usual process operational restrictions. Details of the data for the three vessels (converters) are given in the Table 3.2.

3.3 Data for case study-3: (low initial phosphorous and high MgO in slag)

In case study3, for a 300 ton BOF with bottom stirring, sub-lance is used for in blow measurements. This data set has been classified into three separate groups (as explained in section 3.1) on the basis of additions of ore during 2^{nd} blow (Ore_2) and raw dolomite during 2^{nd} blow (Rdolo2). The details of data sets are given in the Table 3.3.

3.4 Case study-4: Slag morphology and distribution of phosphorous in different phases.

In addition to data for the case studies 1, 2 and 3, slag samples from three more plants have been collected and analyzed on SEM. Two of these plants (with140 ton BOF) have high MgO practice, one with bottom stirring facility and the other not. The third plant (300 ton BOF) has bottom stirring but experiments were conducted with two different operating practices (with and without bauxite additions). The purpose was to see the combined effect of MgO and Al_2O_3 on slag morphology and phosphorous distribution, including the effect of dicalcium silicate (solid fraction) in slags on phosphorous distribution.

Table-3.1 Composition of slag for the data of case study-1

Plant No		Operation-al restriction	Number of data	Composition of slag (average)	Composi-tion of steel	Turn down tempera-ture (^{0}C)
1	Set-1	Ore20 Rdolo2=0	60	%CaO 56, %SiO_2 12 %P_2O_5 1.2, %MnO 3, %MgO 3.5, %FeO 22	[P] 0.011, [C] 0.05, [Mn] 0.15	1599-1705
	Set-2	Ore2=0 Rdolo2=0	110	%CaO 53, %SiO_2 11.8 %P_2O_5 1.2, %MnO 3.2, %MgO 3.3, %FeO 23	[P] 0.011, [C] 0.05, [Mn] 0.15	1630-1708
	Set-3	Ore2=0 Rdolo20	112	%CaO 42.2-65, %SiO_2 12 %P_2O_5 1.2, %MnO 3.2, %MgO 3.3, %FeO 23	[P] 0.011, [C] 0.05, [Mn] 0.15	1610-1699

Table-3.2 Composition of slag for the data of case study-2

Plant		No of data	Composition of slag	Composition of metal	Turn down temperature ^0C
2	Vessel-1	402	%CaO 45-60, $\%SiO_2$ 11-17 $\%P_2O_5$ 3.6, %MnO 0.6, %MgO 0.9, %FeO 18-32	[P] 0.014, [C], 0.03, [Mn] 0.028	1611-1750
	Vessel-2	380	%CaO 56, $\%SiO_2$ 13 $\%P_2O_5$ 3.6, %MnO 0.6, %MgO 0.9, %FeO 22	[P] 0.013, [C] 0.029, [Mn] 0.027	1591-1743
	Vessel-3	270	%CaO 56, $\%SiO_2$ 13 $\%P_2O_5$ 3.5, %MnO 0.6, %MgO 0.9, %FeO 22	[P] 0.013, [C] 0.03, [Mn] 0.027	1601-1741

Table-3.3 Composition of slag for the data of case study-3

Plant No		Operational restriction	Number of data	Composition of slag	Composition of metal	Turn down temperature (^{0}C)
1	Set-1	Ore20 Rdolo2=0	331	%CaO 42, %SiO_2 21.5 %P_2O_5 1.4, %MnO 4, %MgO 8, %FeO 13-30	[P] 0.011, [C] 0.05, [Mn] 0.15	1599-1705
	Set-2	Ore2=0 Rdolo2=0	140	%CaO 42.5, %SiO_2 8-20 %P_2O_5 1.4, %MnO 5, %MgO 8, %FeO13-30	[P] 0 011, [C] 0.05, [Mn] 0.15	1600-1708
	Set-3	Ore2=0 Rdolo20	246	%CaO 44, %SiO_2 8-20 %P_2O_5 0.1.4, %MnO 5, %MgO 8, %FeO 13-30	[P] 0.011, [C] 0.05, [Mn] 0 15	1610-1699

CHAPTER-4

Application of thermodynamic models to predict phosphorous in steel at tap

4.0 Introduction :

The thermodynamic models discussed in chapter 2 have been tested and tuned for different data sets (described in chapter 3). The results observed after tuning are reported here (section 4.1-4.3) As mentioned earlier, low phosphorous hot metal has <0.07% P and high phosphorous hot metal has 0.2-0.26% P. Low MgO practice means less than 2% MgO in final slag and high MgO practice means 7-11% MgO in final slag.

4.1 Results of case studies 1, 2, and 3:

The attempt here is to predict end point phosphorous in steel when slag analysis is calculated from mass balance on the basis of the charge materials. It is therefore not necessary to take slag sample at tap and wait for the analysis to arrive, which is time consuming and some times impractible.

4.1.1 Result of case study-1: low phosphorous containing hot metal and low MgO slag practice.

In this case study, different models were tested for the three different cases of data sets as described in section 3.1. In set 1 Ore is added during the 2^{nd} blow but raw dolomite is not added during the 2^{nd} blow. In set-2 neither ore nor raw dolomite is added during the 2^{nd} blow. In set-3 raw dolomite is added during the 2^{nd} blow but ore is not added during the 2^{nd} blow.

The following equations (listed in Table 4.1) are obtained for different sets of data in case study-1 by incorporating additional variables HL_2, HTR, C_2, Ore_2, T_2, and SVO into Healy's model, molecular theory model, optical basicity model and quadratic formalism model. The corresponding product moment correlation coefficient (R) standard error of estimate (σ) is also indicated.

Table-4.1 Summary of result of application of different models for data set-1, 2 and 3 (Case study-1)

A: Application of Healy's model for data set-1, 2 and 3 (case study-1).				
Data set	Equation	R	σ	Equation No
Set-1 for case study-1	$\log\frac{(P)}{[P]}=\frac{19830.24}{T_2}+0.0024\times HL_2-9.03\times C_2+0.018\times(CaO)$ $+3.98\times10^{-5}\times SVO+8.77\times10^{-5}\times ORE_2-9.78$	0.72	0.0024	E.q-4.1
Set-2 for case study-1	$\log\frac{(P)}{[P]}=\frac{14922.77}{T_2}+0.00078\times HL_2$ $-10.34\times C_2+0\ 011\times(CaO)-6.22$	0.65	0.0023	E.q-4.2
Set-3 for case study-1	$\log\frac{(P)}{[P]}=\frac{221804.73}{T_2}+0.0014\times HL_2-8.6\times C_2$ $+0.0135\times(CaO)+3.9\times10^{-6}SVO-10.31$	0.81	0.0033	E.q-4.3
B: Application of Molecular theory model for data set-1, 2 and 3 (case study-1).				
Data set	Equation	R	σ	Equation No
Set-1 for case study-1	$\log\frac{(P)}{[P]^2}=\frac{29641.7}{(T_2-255.22)}+0.0043\times HL_2-18\ 37\times C_2$ $+4.75\times\log(CaO)+1.9\times10^{-5}\times SVO+0.00017\times Ore_2-22.9$	0.74	0.0021	E.q-4.4
Set-2 for case study-1	$\log\frac{(P)}{[P]^2}=\frac{22986.1}{(T_2-255.22)}-20.37\times C_2+2.6\times\log(CaO)$ $+9.29\times10^{-6}\times SVO-13.79$	0.67	0.0023	E.q-4.5
Set-3 for case study-1	$\log\frac{(P)}{[P]^2}=\frac{30914.95}{(T_2-255\ 22)}+0\ 033\times HL_2-14.96\times C_2$ $+1.61\times\log(CaO)+1\ 38\times10^{-5}\times SVO+0\ 029\times HTR-18\ 03$	0.81	0.0035	E.q-4.6

Table 4.1 continued.....

Table-4.1 Summary of result of application of different models for data set-1, 2 and 3 (Case Study-1)

C: Application of optical basicity model for data set-1, 2 and 3 (cast study-1)				
Data set	Equation	R	σ	Equation No
Set-1 for case study-1	$\log\frac{(P)}{[P]}=\frac{12967.3}{T_2}+0.0025\times HL_2+0.00015\times Ore_2-5.58$	0.67	0.0021	E.q-4.7
Set-2 for case study-1	$\log\frac{(P)}{[P]}=\frac{12689.7}{T_2}+0.00091\times HL_2-4.9\times C_2-4.76$	0.69	0.0022	E.q-4.8
Set-3 for case study-1	$\log\frac{(P)}{[P]}=\frac{18023.84}{T_2}+0.0015\times HL_2-4.92\times C_2-1.01\times\wedge-6.85$	0.77	0.003	E.q-4.9
D: Application of quadratic formalism model for data set-1, 2 and 3 (case study-1).				
Data set	Equation	R	σ	Equation No
Set-1 for case study-1	$RT\ln[P]=176.38\times T_2-53.19\times HL_2+222517.09\times C_2$ $-0.42\times SVO-4.5\times Ore_2+0.08\times RT\ln(a_{P_2O_5})-334997$	0.74	0.0021	E.q-4.10
Set-2 for case study-1	$RT\ln[P]=124.93\times T_2+245700.4\times C_2-0.24\times SVO$ $+0.089\times RT\ln(a_{P_2O_5})-252990.28$	0.68	0.0018	E.q-4.11
Set-3 for case study-1	$RT\ln[P]=196.44\times T_2-34.14\times HL_2+210671\times C_2$ $-0.31\times SVO+0.07\times RT\ln(a_{P_2O_5})-390571$	0.74	0.0027	E.q-4.12

The result in the Table .1 shows that molecular theory model, on the basis of R and σ values, is best suited for case study-1 (for more details regarding 't' values reference may be made to Table 4.5, 4.6 and 4.7 for set-1, 2 and 3, respectively).

4.1.2 Result of case study-2: High phosphorous in hot metal and low (MgO) in slag practice.

The following equations (listed in Table 4.2) are obtained for different sets of data in case study-2 by incorporating additional variables HTR, C_2, Ore, T_2, and SVO into the different models.

Table 4.2 Summary of result of application of different models for vessel 1, 2 and 3 (Case study-2)

A: Application of Healy's model for vessel-1, 2 and 3 (case study-2).				
Data set	Equation	R	σ	Equation No
Vessel-1 for case study-2	$\log\frac{(P)}{[P]} = -0.023\times T_2 - 0.77\times C_2 + 0.01\times(CaO) + 0.004\times Ore) + 6.01$	0.65	0.0018	E.q-4.13
Vessel-2 for case study-2	$\log\frac{(P)}{[P]} = -0.019\times T_2 + 0.99\times C_2 + 0.0057\times(CaO) + 0.04\times Ore + 5.59$	0.61	0.0017	E.q-4.14
Vessel-3 for case study-2	$\log\frac{(P)}{[P]} = -0.019\times T_2 + 0.99\times C_2 + 0.0057\times(CaO) + 0.004\times ORE + 5.59$	0.66	0.0016	E.q-4.15

Table 4.2 continued.....

Table-4.2 Summary of result of application of different models for vessel 1, 2 and 3 (Case study-2)

B: Application of Molecular theory model for vessel-1, 2 and 3 (case study-2).

Data set	Equation	R	σ	Equation No
Vessel-1 for case study-2	$\log\frac{(P)}{[P]}=\frac{11953.49}{(T_2-255.22)}+0.0082\times\log(CaO)$ $+0.041\times SVO+1.57\times\log(Fe)-6.09$	0.79	0.0027	E.q-4.16
Vessel-2 for case study-2	$\log\frac{(P)}{[P]^2}=\frac{11009.93}{(T_2-255.22)}+2.95\times\log(CaO)$ $+0.0041\times SVO+0.74\times\log(Fe)-8.6$	0.66	0.0016	E.q-4.17
Vessel-3 for case study-2	$\log\frac{(P)}{[P]^2}=\frac{9210.33}{(T_2-255.22)}+1.8\times C_2+0.01\times ORE-1.5$	0.62	0.0015	E.q-4.18

C: Application of optical basicity model for vessel-1, 2 and 3 (cast study-2)

Data set	Equation	R	σ	Equation No
Vessel-1 for case study-2	$\log\frac{(P)}{[P]}=-0.0015\times T_2+0.0062\times ore+2.26\times\wedge+3.16$	0.5	0.0063	E.q-4.19
Vessel-2 for case study-2	$\log\frac{(P)}{[P]}=-0.0019\times T_2-0.711\times C_2+5.9$	0.63	0.0017	E.q-4.20
Vessel-3 for case study-2	$\log\frac{(P)}{[P]}=-0.018\times T_2+0\ 88\times C_2+0.0045\times\wedge+5.58$	0.6	0.0016	E.q-4.21

Table 4.2 continued.....

Table-4.2 Summary of result of application of different models for data vessel 1, 2 and 3 (Case study-2)

D: Application of quadratic formalism model for vessel-1, 2 and 3 (case study-2).				
Data set	Equation	R	σ	Equation No
Vessel-1 for case study-2	$RT\ln[P] = T_2 \times 30.89 - 188.35 \times Ore$ $-301.48 \times SVO - 0.012 \times RT\ln[O] - 1126277$	0.66	0.0016	E.q-4.22
Vessel-2 for case study-2	$RT\ln[P] = 63.18 \times T_2 - 12641 \times RT\ln[O]$ $-30.46 \times SVO - 1370.76 \times basicity - 197106.26$	0.52	0.0063	E.q-4.23
Vessel-3 for case study-2	$RT\ln[P] = -0.045 \times RT\ln(K_p)$ $-181.475 \times Ore - 141.32 \times SVO - 85772.9$	0.68	0.0013	E.q-2.24

(For more details regarding 't' values reference may be made to Table 4.7, 4.8 and 4 9 for vessel 1, 2 and 3 respectively). Simular to the results for case study-1, it is found that molecular theory model is appropriate (on the basis of R and σ values) for case study 2 as well.

In section 4.1-4.2, out of the different models tested for different data sets with different operating conditions, it is observed that the molecular theory model gives the best prediction of end point phosphorous in most of the cases Therefore only molecular theory model has been tried for case study-3, which is described in the next section below.

4.1.3 Result of case study-3: Low phosphorous in hot metal and high MgO in slag practice.

In this case study molecular theory model is tested for the three different cases of data sets described in chapter 3 (details of data sets are given in Table 4.3). In set 1 Ore is added during 2nd blow but raw dolomite is not added during 2nd blow. In set-2 neither ore nor raw dolomite added during 2nd blow. In set-3 raw dolomite is added during 2nd blow but ore is not added during 2nd blow.

The following equations are obtained for different sets of data in case study-3 when MLR is carried out by incorporating the additional variables C_2, SVO, Ore2, HL_2, T_2, Basicity and HTR in the original molecular theory model.

Table-4.3 Summary of result of application of different models for data set-1, 2 and 3 (Case study-3)

Data set	Equation	R	σ	Equation No
Set-1 for case study-3	$\log\frac{(P)}{[P]^2}=\frac{25610.1}{(T_2-255.22)}+1.74\times C_2+.0036\times SVO$ $+0.074\times Basicity-11.89$	0.69	0.0025	E.q-4.25
Set-2 for case study-3	$\log\frac{(P)}{[P]^2}=\frac{20178.01}{(T_2-255.22)}+1.097\times\log(CaO)-10.04$	0.59	0.0019	E.q-4.26
Set-3 for case study-3	$\log\frac{(P)}{[P]^2}=\frac{27718.3}{(T_2-255.22)_2}+4.35\times C_2+0.58\times\log(CaO)$ $+5.07\times10^{-5}\times Rdolo_2-13.96$	0.76	0.001	E.q-4.27

(For more details regarding 't' values reference may be made to Table 4.10).In all the above equations, coefficients of $\frac{1}{(T_2-255.22)}$, log(CaO), SVO, Basicity are positive

which is expected from thermodynamic consideration. However, the positive coefficient of turn down carbon is not expected from thermodynamic considerations.

4.2 Discussion: individual effects if different variables on phosphorous distribution.

It is first interesting to compare the sign of the coefficient of the different parameters for the best selected models in each set as shown Table 4.14.

Table-4.4 Comparison of individual effects of different variables on phosphorous distribution.

Sign of the coefficient of selected variables for molecular theory model of three case study													
Data Set	Variables												
	T_2	$\frac{1}{(T_2-255\,22)}$	Log (CaO)	Log (Fe)	C_2	SVO	Basicity	C_2S	Ore	HTR	Hl_2	Ore_2	$Rdolo_2$
1		+	+		-	+					+	+	
2		+	+		-	+							
3		+	+		-	+				+	+		
1		+	+			+	+		+				
2		+	+	+		+							
3		+			+				+				
1		+	+		+	+	+						
2		+	+										
3		+	+		+								+

(a) Effect of turndown temperature ($\frac{1}{(T_2-255.22)}$):

The parameter $\frac{1}{(T_2-255.22)}$ has been selected in the regression equation in all cases and its coefficient is positive. It implies that turndown temperature is a significant variable for dephosphorisation and the effect of turndown temperature is negative on dephosphorisation.

(b) Effect of log(CaO) :

Log(CaO) is a significant parameter for molecular theory model and it has been selected for eight out of the nine cases in the Table-4.4. Coefficient of log(CaO) is positive, it implies that effect of (CaO) is positive on dephosphorisation.

(c) Effect of basicity:

Basicity is known to be a significant parameter, although it is selected only in 2 out of 9 equations in Table 4.4. Its coefficient is positive. The fact that it is selected only in 2 out of 9 cases may be due to the limited variation in basicity range itself.

(d) Effect of slag mass:

Slag mass is a significant parameter in 6 out of 9 cases. Its coefficient is positive. Hence the effect of slag mass is positive on dephosphorisation.

(e) Effect of total amount ore added:

Total amount of ore added is a significant parameter in 2 out of 9 cases. Its coefficient is positive. It implies that increasing the amount of total ore may improve dephosphorisation.

(f) Effect of lance height during second blow (Hl_2):

Coefficient of Hl_2 is positive for the 2 cases (Table-4.4) where it has been selected as a parameter. Which means increasing lance height during 2^{nd} blow will improve dephosphorisation.

(g) Effect of log(Fe):

Coefficient of log(Fe) is positive in one case (Table-4.4). It is observed that log(Fe) is not a selected parameter in those cases where Hl_2 is selected as a parameter. This is because log(Fe) and Hl_2 are related parameters.

(h) Effect of ore added during second blow (Ore2):

Ore 2 has been selected only in two cases in Table-4.4. Its coefficient is positive. It implies that if we increase the amount of ore addition during the 2^{nd} blow, dephosphorisation may improve.

(i) Effect of carbon at tap (C_2):

Coefficient of C_2 is negative for the data sets of case study-1 (for the low MgO (<2%) slag and low phosphorous (<0.06%) in hot metal practice). For high MgO slag the coefficient of C_2 is positive. This may be due to the effect of MgO on viscosity of slag.

(j) Effect of HTR:

HTR is not a selected parameter it implies that HTR is not important parameter for dephosphorisation, for the case studies selected in this work.

Table 4.5 Summary of 't' values for significant variables of different models (for dataset 1 of case study-1).

Operational constraint				Additional variable for tuning		
$Ore_2$0, $Rdlo_2$=0				Ore_2, Hl2, T_2, SVO, C_2, HTR		
Model	Dependent variable	Variables selected		Variables rejected	R	σ
		Variables	(t) value for selected variables			
Modified Healy's model	$\log\frac{(P)}{[P]}$	$\frac{1}{T_2}$	5.7	HTR, log(Fe), T_2	0.72	0.0024
		Hl_2	2.99			
		C_2	-4.5			
		(CaO)	6.5			
		SVO	1.7			
		Ore_2	1.47			
Modified molecular theory model	$\log\frac{(P)^2}{[P]}$	$\frac{1}{(T_2-255.22)}$	6.6	HTR, log(Fe), T_2	0.74	0.0021
		Hl_2	2.75			
		Ore_2	1.75			
		SVO	3.67			
		log(CaO)	4.65			
		C_2	-4.42			
Modified optical basicity model	$\log\frac{(P)}{[P]}$	$\frac{1}{T_2}$	5.35	HTR, OB, SVO, T_2, log(Fe), C_2	0.70	0.0021
		Ore_2	1.98			
		Hl_2	2.68			
Modified quadratic formalism model	RTln[P]	Ore_2	-2.6	HTR, Rtln[O] , RTln[K_P]	0.74	0.0021
		SVO	-5.04			
		C_2	3.28			
		$RT\ln(a_{P_2O_5})$	2.5			
		HL_2	-1.8			
		T2	4.8			

Table 4.6 Summary of 't' values for significant variables (dataset 2 of case study-1).

Operational constraint				Additional variable for tuning		
Ore_2=0, $Rdolo_2$=0				$Dolo_2$, Hl2, T_2, SVO, C_2, HTR		
Model	Dependent variable	Variables selected		Variables rejected	R	σ
		Variables	(t) value for selected variables			
Modified Healy's model	$\log\frac{(P)}{[P]}$	$\frac{1}{T_2}$	5.9	HTR, (%CaO), T_2, Hl_2, SVO, dolo2	0.72	0.0023
		HL_2	6.5			
		C_2	-5.4			
		(CaO)	2.66			
Modified molecular theory model	$\log\frac{(P)^2}{[P]}$	$\frac{1}{(T_2-255.22)}$	6.06	HTR, T_2, dolo2, Hl_2, log(Fe)	0.67	0.0023
		C_2	-5.48			
		log(CaO)	1.4			
		SVO	2.9			
Modified optical basicity model	$\log\frac{(P)}{[P]}$	$\frac{1}{T_2}$	5.13	HTR, OB, SVO, Hl_2. $dolo_2$	0.69	0.0022
		Hl2	1.99			
		C_2	-3 4			
Modified quadratic formalism model	RTln[P]	$RT\ln(a_{P_2O_5})$	1.85	HTR, Hl_2, RTln[O], $Dolo_2$, HTR, $RT\ln(K_P)$	0.68	0.0018
		SVO	-3.85			
		T_2	5.27			
		C2	2.48			

Table 4.7 Summary of 't' values for significant variables (dataset 3 of case study-1).

Operational constraint				Additional variable for tuning		
Ore_2=0, $Rdolo_2$0				Hl_2, T_2, SVO, C_2, HTR		
Model	Dependent variable	Variables selected		Variables rejected	R	σ
		Variables	(t) value for selected variables			
Modified Healy's model	$\log\frac{(P)}{[P]}$	$\frac{1}{T_2}$	12.55	HTR, T_2, , Log(Fe)	0.81	0.0033
		Hl_2	3.34			
		C_2	-7.16			
		(%CaO)	5.6			
		SVO	3.42			
Modified molecular theory model	$\log\frac{(P)^2}{[P]}$	$\frac{1}{(T_2-255.22)}$	11.33	T_2, log(Fe), HTR	0.81	0.0036
		HL2	3.58			
		C_2	-4.95			
		log(CaO)	3.47			
		SVO	4.33			
Modified optical basicity model	$\log\frac{(P)}{[P]}$	$\frac{1}{T_2}$	9.56	HTR, SVO, log(Fe)	0.76	0.0033
		Hl_2	3.43			
		C_2	-4.48			
		OB	-1.67			
Modified quadratic formalism model	RTln[P]	SVO	-5.5	HTR, RTln(K_P), RTln[O]	0.74	0.0027
		T2	9.4			
		C2	4.7			
		$RT\ln(a_{P_2O_5}$	3.5			
		Hl2	-2.2			

Table 4.8 Summary of 't' values for significant variables (vessel-1 of case study-2).

High phosphorous hot metal Low MgO slag				Additional variable for tuning T_2, SVO, C_2, HTR, Ore, Basicity		
Model	Dependent variable	Variables selected		Variables rejected	R	σ
		Variables	(t) value for selected variables			
Modified Healy's model	$\log\frac{(P)}{[P]}$	T_2	-14 23	HTR, log(Fe) Basicity, $\frac{1}{T_2}$	0.8	0.0028
		(%CaO)	5 884			
		C2	-2.23			
		Ore	1.96			
Modified molecular theory model	$\log\frac{(P)}{[P]^2}$	$\frac{1}{(T_2-255.22)}$	-1.69	HTR, Basicity, C_2	0.79	0.0027
		T_2	-2.19			
		log(CaO)	4.7			
		SVO	2.18			
		Ore	3.34			
		Log(Fe)	3.69			
Modified optical basicity model	$\log\frac{(P)}{[P]}$	T_2	-9.01	HTR, SVO, $\frac{1}{T_2}$, C_2	0.5	0.0063
		Ore	3.43			
		OB	4.14			
Modified quadratic formalism model	RTln[P]	SVO	-4.39	HTR, TDC, RTln[O], HTR, $RT\ln(K_P)$	0.66	0.0016
		$RT\ln(a_{P_2O_5})$	-1.65			
		Ore	-2.26			
		T_2	4.6			

Table 4.9 Summary of 't' values for significant variables (vessel-2 of case study-2).

High hot metal phosphorous. Low MgO slag				Additional variable for tuning T_2, SVO, C_2, HTR, Ore, Basicity		
Model	Dependent variable	Variables selected		Variables rejected	R	σ
Modified Healy's model	$\log\frac{(P)}{[P]}$	Variables	(t) value for selected variables			
		C_2	-1.5	HTR, SVO, $\frac{1}{T_2}$, Basicity, log(Fe).	0.61	0.00017
		(%CaO)	6 097			
		T_2	-14.6			
		Ore	2.01			
Modified molecular theory model	$\log\frac{(P)^2}{[P]}$	$\frac{1}{(T_2-255.22)}$	14.6	HTR, Basicity, C_2, Ore, T_2	0.66	0.0016
		log(CaO)	3.6			
		SVO	1.86			
		Log(Fe)	2.08			
Modified optical basicity model	$\log\frac{(P)}{[P]}$	T_2	-14.7	HTR, SVO, $\frac{1}{T_2}$, log(Fe),Ore	0.63	.0017
		C_2	-2.1			
Modified quadratic formalism model	RTln[P]	$RT\ln(a_{P_2O_5})$	-1.65	HTR, C_2 ,RTln[O], HTR, RTln(K_P), SVO	0.52	0.0063
		Ore	4.6			
		T_2	-2.26			

Table 4.10 Summary of 't' values for significant variables (vessel-3 of case study-2).

High hot metal phosphorous. Low MgO slag				Additional variable for tuning T_2, SVO, C_2, HTR, Ore, Basicity		
Model	Dependent variable	Variables selected		Variables rejected	R	σ
Modifies Healy's model	$\log\frac{(P)}{[P]}$	Variables	(t) value for selected variables			
		TDC	2.3	(CaO), SVO, $\frac{1}{T_2}$, HTR Basicity, log(Fe)	0.66	0.0017
		(CaO)	2.7			
		Ore	2.5			
		T_2	-12.3			
Modified molecular theory model	$\log\frac{(P)^2}{[P]}$	$\frac{1}{(T_2 - 255\ 22)}$	9.12	HTR, Basicity, T_2, SVO, log(Fe), log(CaO)	0.62	0.0015
		Ore	2.86			
		C_2	1.91			
Modified optical basicity model	$\log\frac{(P)}{[P]}$	TDC	2.06	HTR, SVO, $\frac{1}{T_2}$, TDC, OB, log(Fe)	.6	0.016
		T_2	-11.8			
		OB	2.6			
Modified quadratic formalism model	RTln[P]	$RT\ln(K_P)$	-4.23	HTR, $\frac{1}{T_2}$, TDC, basicity, $RT\ln(a_{P_2O_5})$ RTln[O]	.65	00013
		Ore	-2.45			
		SVO	-2.096			

Table 4.11 Summary of 't' values for significant variables (case study 3).

High MgO (7-11%) in slag and low phosphorous (<0.07%) hot metal				Additional variable for tuning T_2, SVO, C_2, HTR, Ore, Basicity		
Data set	Dependent variable	Variables selected		Variables rejected	R	σ
		Variables	(t) value for selected variables			
Set-1	$\log\frac{(P)}{[P]^2}$	$\frac{1}{(T_2-255.22)}$	18 91	HTR, Ore2, Hl2, Log(Fe), log(CaO)	0.69	0.0025
		C_2	1.93			
		Basicity	2 10			
		SVO	1.55			
Set-2	$\log\frac{(P)}{[P]^2}$	$\frac{1}{(T_2-255.22)}$	6.36	HTR, Log(Fe), Basicity, HTR, SVO	0.59	0.0019
		Log(CaO)	2.4			
Set-3	$\log\frac{(P)}{[P]^2}$	$\frac{1}{(T_2-255.22)}$	15 01	HTR, , , Log(Fe), log(CaO), basicity,	0.76	0.0017
		c2	3 5			
		rdlo2	2 5			
		Log(CaO)	1 35			

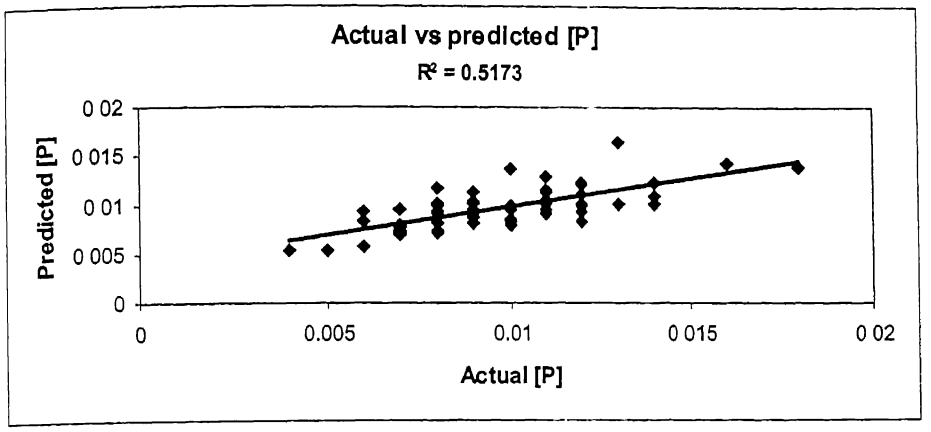

Fig 4.1 Comparison between actual and predicted phosphorous at the end of blow by modified Healy's model for set-1 of case study-1 (Eq. 4.1)

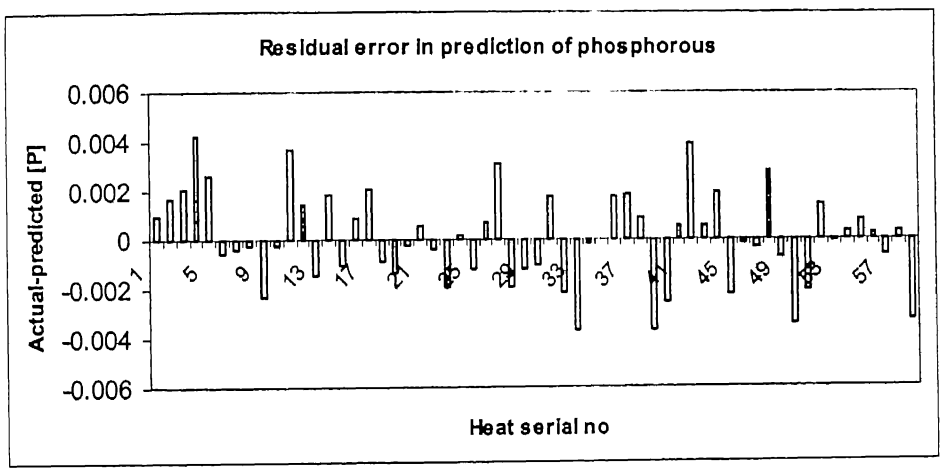

Fig 4.2 Residual error plot for prediction of turndown phosphorous by modified Healy's model for set-1 of case study-1 (E q4.1)

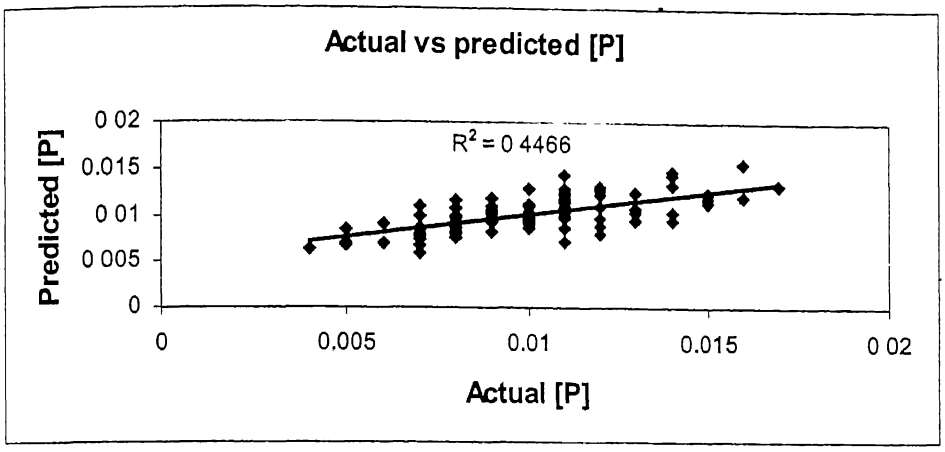

Fig 4.3 Comparison between actual and predicted phosphorous at the end of blow by modified Healy's model for set-2 of case study-1 (Eq. 4.2)

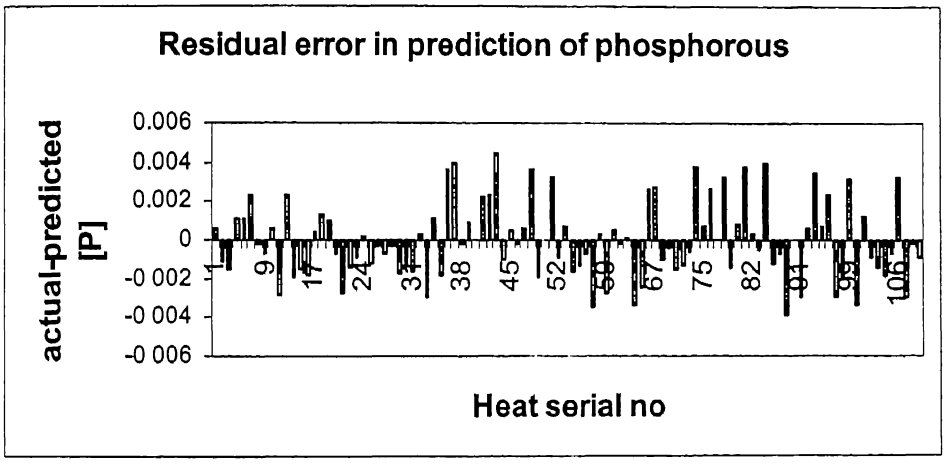

Fig 4.4 Residual error plot for prediction turndown phosphorous by modified Healy's model for set-2 of case study-1 (Eq. 4.2)

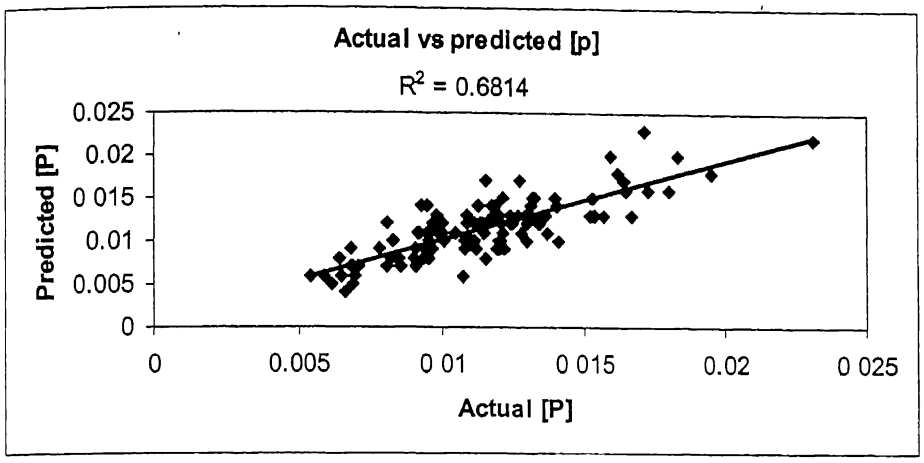

Fig 4.5 Comparison between actual and predicted phosphorous at the end of blow by modified Healy's model for set-3 of case study-1 (Eq. 4.3)

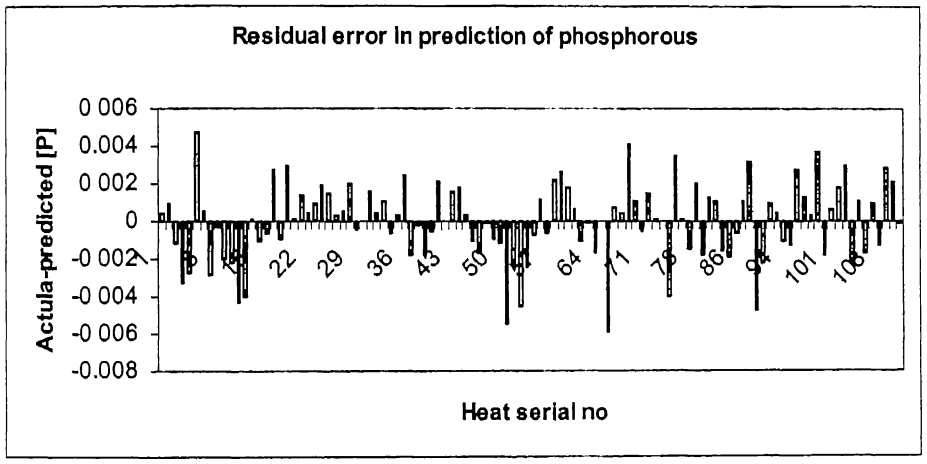

Fig4.6 Residual error plot for prediction of turndown phosphorous by modified Healy's model for set-3 of case study-1 (Eq. 4.3)

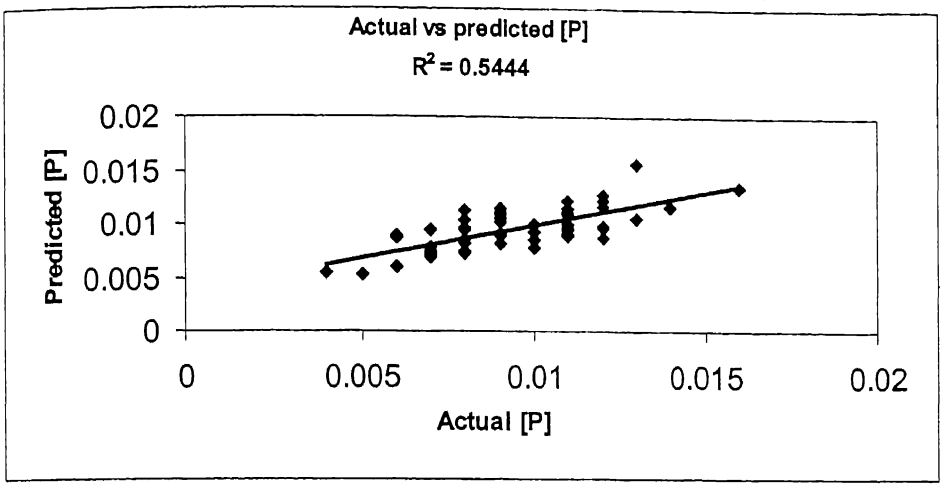

Fig 4.7 Comparison between actual and predicted phosphorous at the end of blow by modified molecular theory model for set-1 of case study-1 (Eq. 4.4)

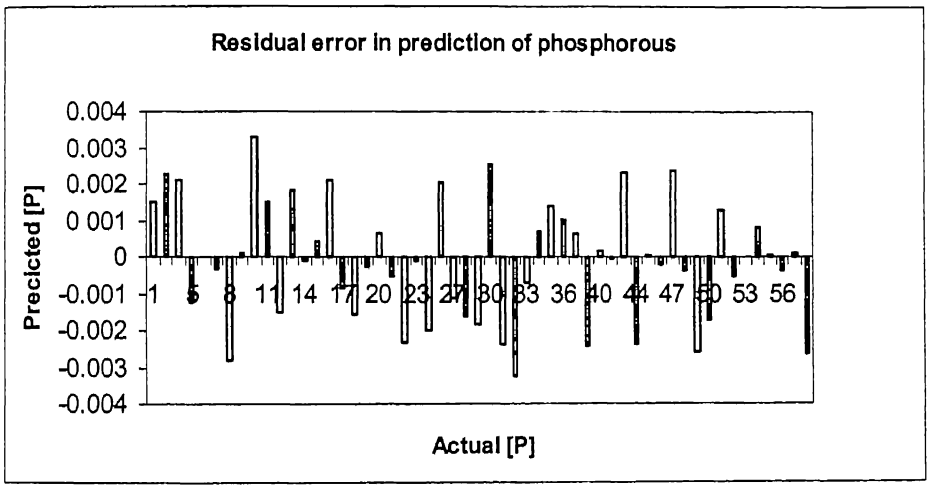

Fig 4.8 Residual error plot for prediction of turndown phosphorous by modified Molecular theory model for set-1 of case study-1 (Eq. 4.4)

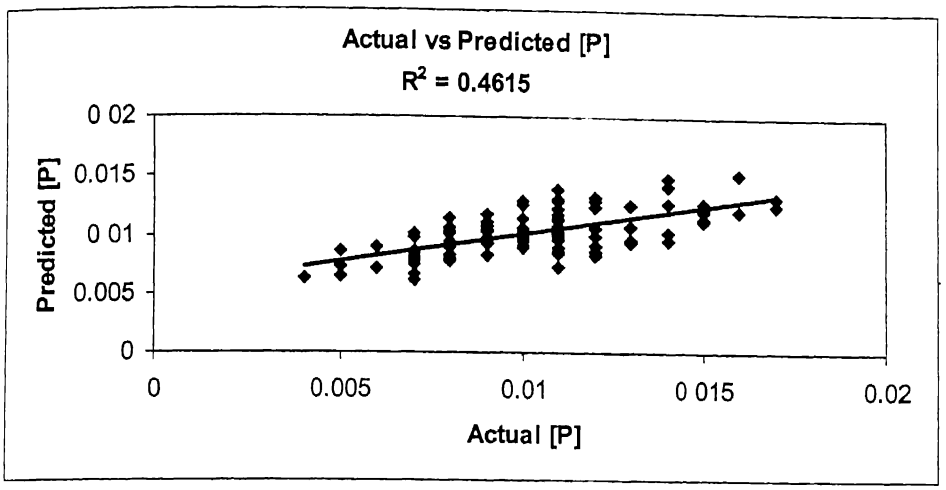

Fig 4.9 Comparison between actual and predicted phosphorous at the end of blow by modified molecular theory model for set-2 of case study-1 (Eq. 4.5)

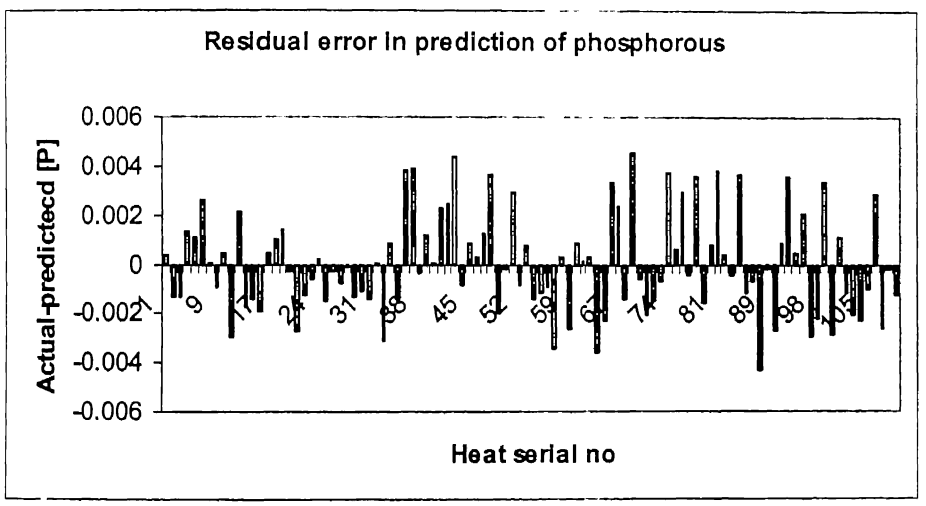

Fig 4.10 Residual error plot for prediction of turndown phosphorous by modified Molecular theory model for set-2 of case study-1 (Eq. 4.5)

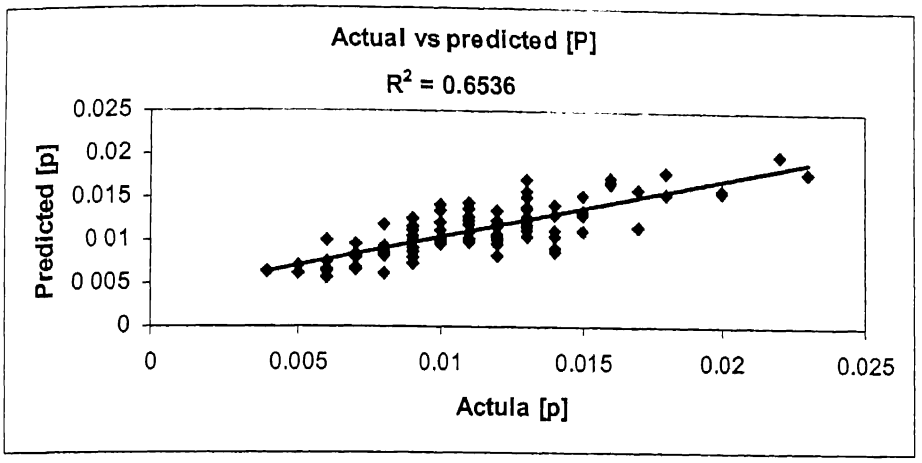

Fig 4.11 Comparison between actual and predicted phosphorous at the end of blow by modified molecular theory model for set-3 of case study-1 (Eq. 4.6)

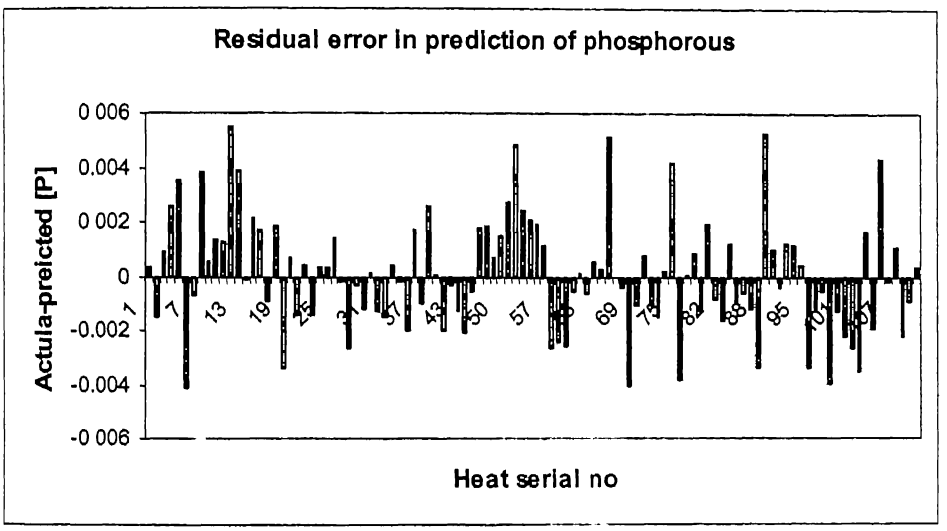

Fig 4.12 Residual error plot for prediction of turndown phosphorous by modified Molecular theory model for set-3 of case study-1 (Eq4.6)

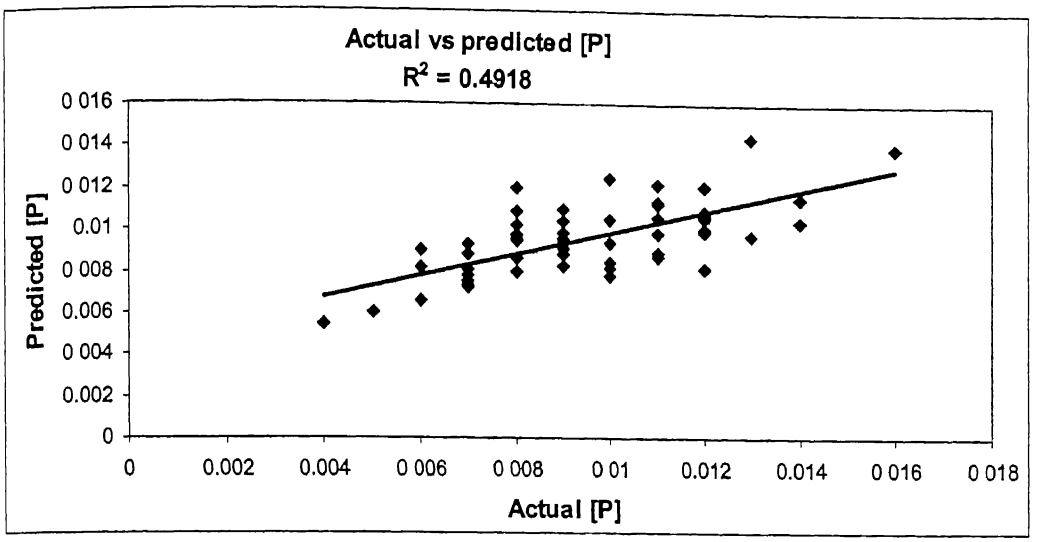

Fig4.13 Comparison between actual and predicted phosphorous at the end of blow by modified optical basicity model for set-1 of case study-1 (Eq4.7)

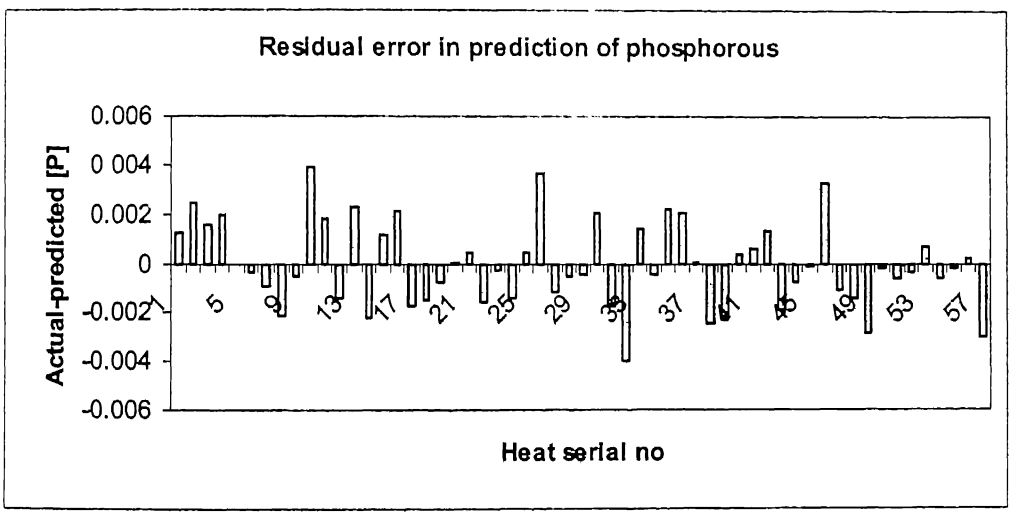

Fig 4.14 Residual error plot for prediction of turndown phosphorous by modified optical basicity model for set-1 of case study-1 (Eq. 4.7)

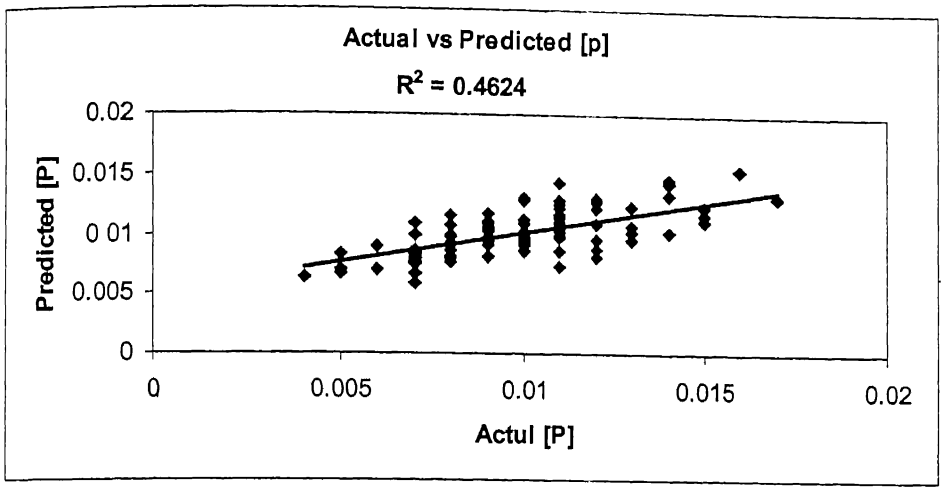

Fig 4.15 Comparison between actual and predicted phosphorous at the end of blow by modified Optical basicity model for set-2 of case study-1 (Eq4.8)

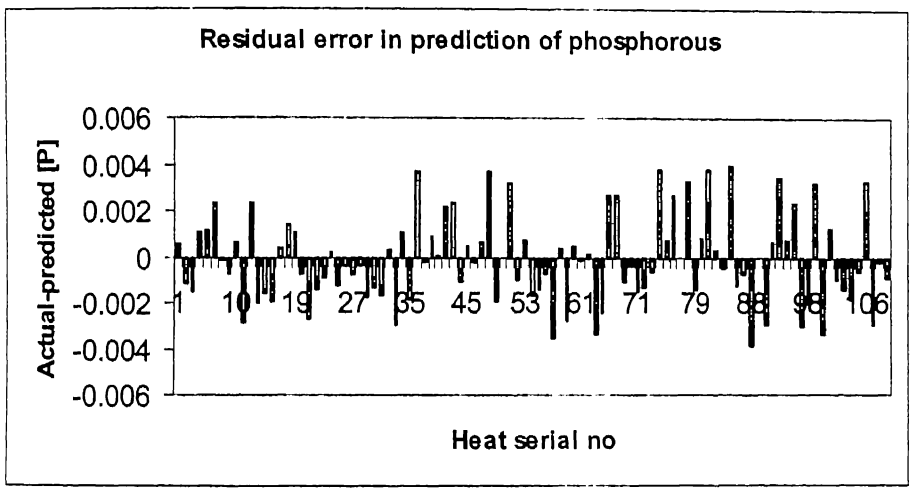

Fig 4.16 Residual error plot for prediction of turndown phosphorous by equation modified optical basicity model for set-2 of case study-1 (Eq. 4.8).

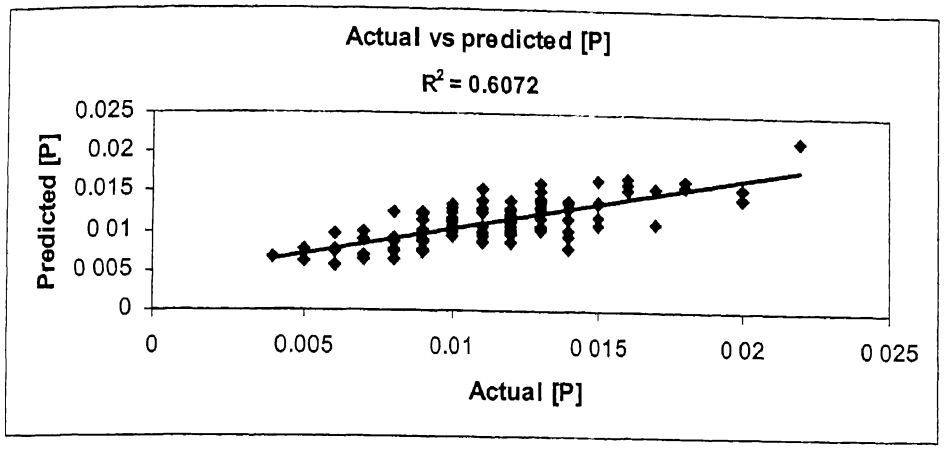

Fig 4.17 Comparison between actual and predicted phosphorous at the end of blow by modified optical basicity model for set-3 of case study-1 (Eq. 4.9)

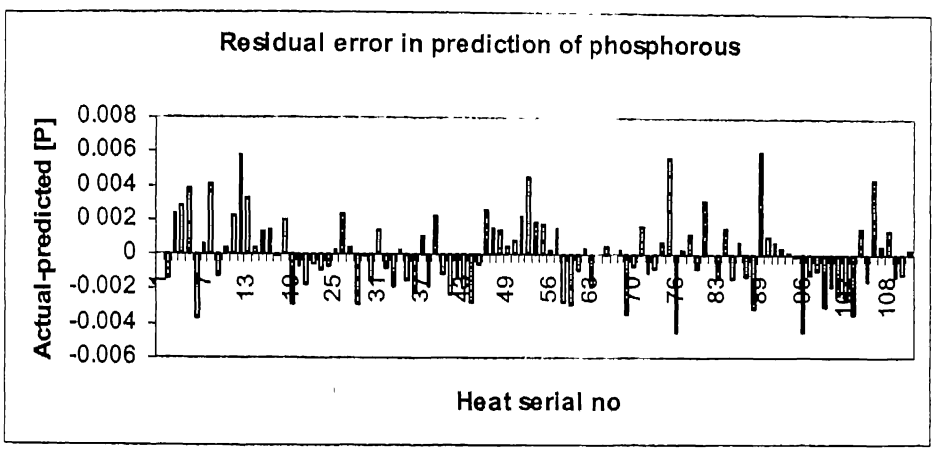

Fig 4.18 Residual error plot for prediction of turndown phosphorous by modified optical basicity model for set-3 of case study-1 (Eq. 4.9)

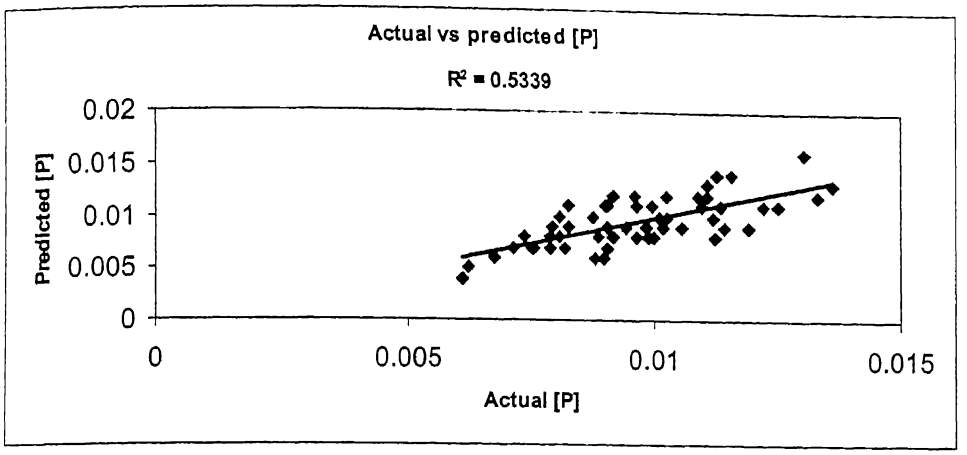

Fig4.19 Comparison between actual and predicted phosphorous at the end of blow by modified quadratic formalism model for set-1 of case study-1 (Eq. 4.10)

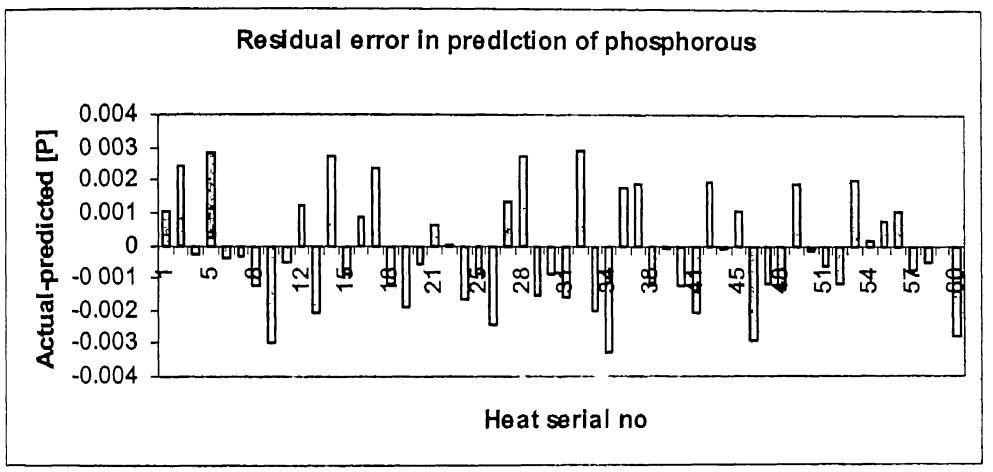

Fig 4.20 Residual error plot for prediction of turndown phosphorous modified quadratic formalism model for set-1 of case study-1 (Eq. 4.10)

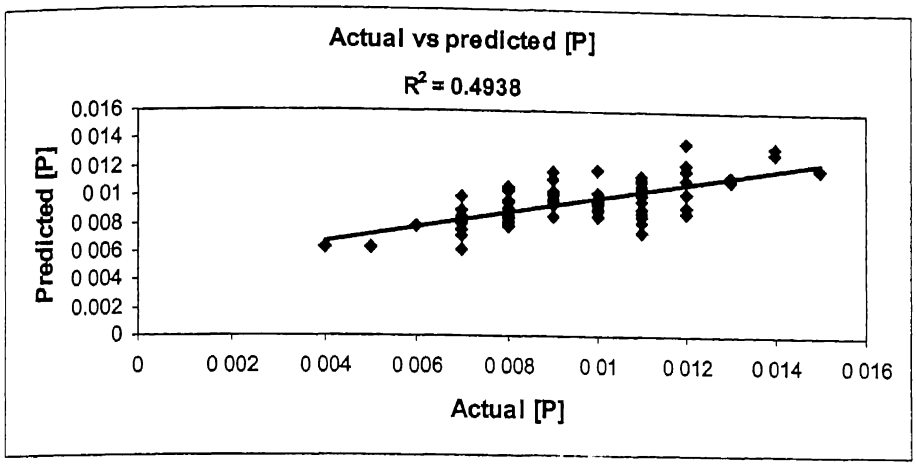

Fig 4.21 Comparison between actual and predicted phosphorous at the end of blow by modified quadratic formalism model for set-2 of case study-1 (Eq. 4.11)

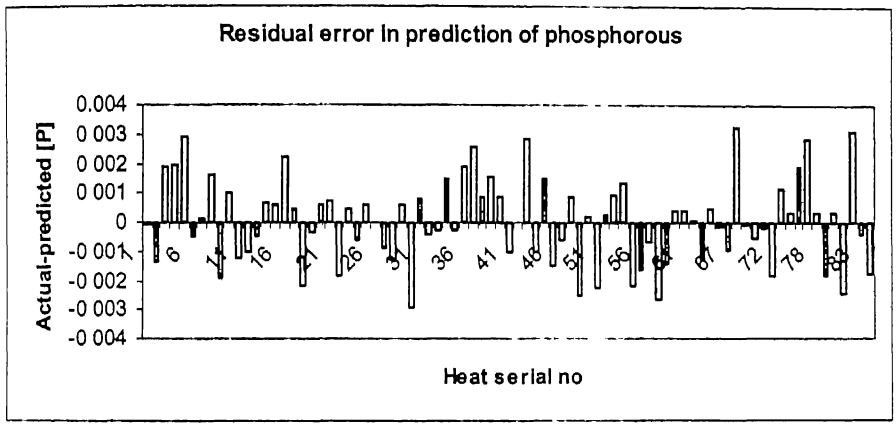

Fig 4.22 Residual error plot for prediction of turndown phosphorous by modified quadratic formalism model for set-2 of case study-1 (Eq. 4.11)

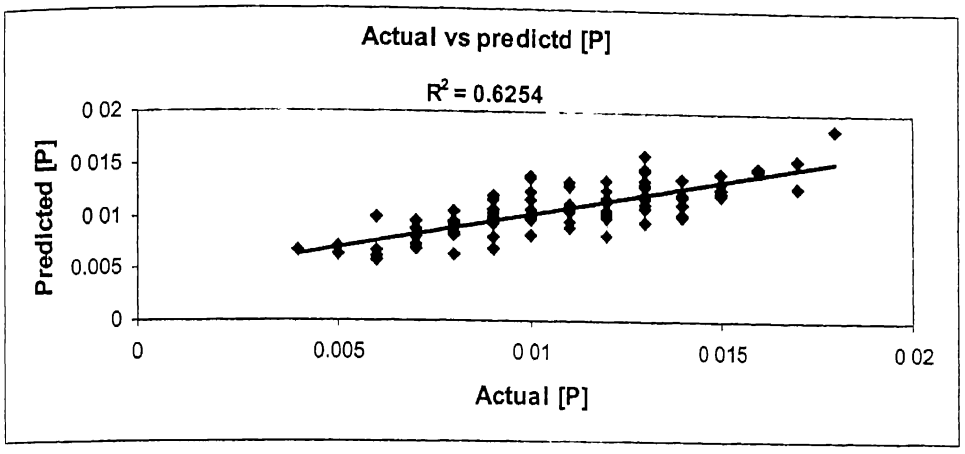

Fig 4.23 Comparison between actual and predicted phosphorous at the end of blow by modified quadratic formalism model for set-3 of case study-1 (Eq. 4.12)

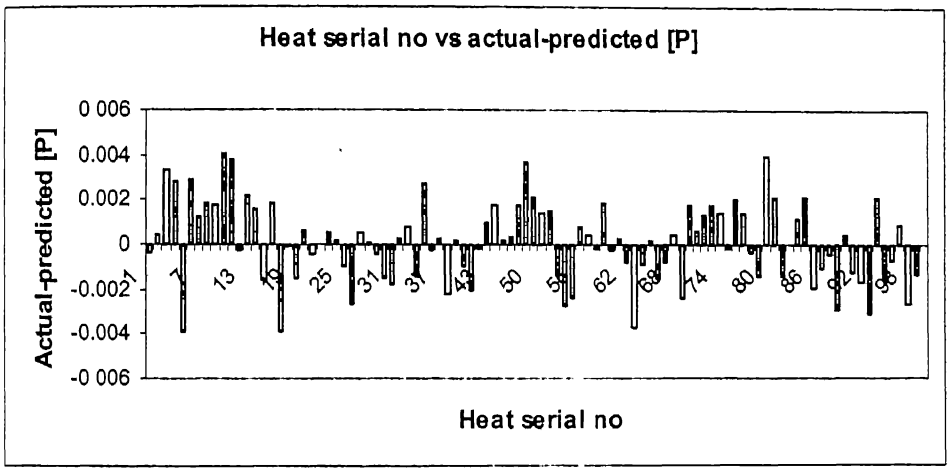

Fig4.24 Residual error plot for prediction of turndown phosphorous by modified quadratic formalism model for set-3 of case study-1 (Eq. 4.12)

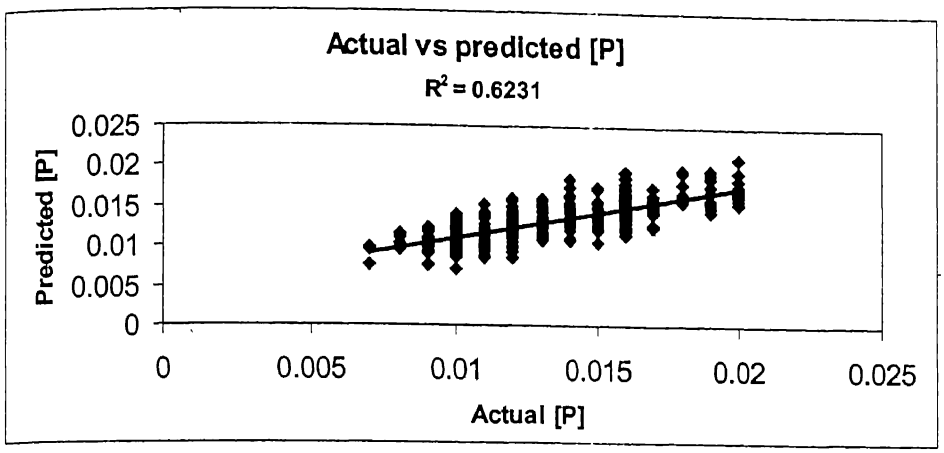

Fig4.25 Comparison between actual and predicted phosphorous at the end of blow by modified Healy's model for vessel-1 of case study-2 (Eq. 4.13)

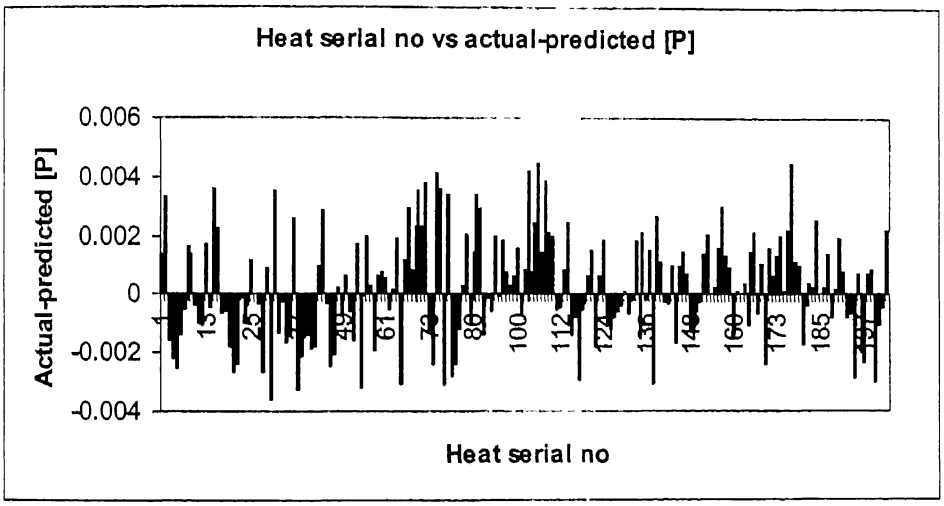

Fig 4.26 Residual error plot for prediction of turndown phosphorous by modified Healy's model for vessel-1 of case study-2 (Eq. 4.13)

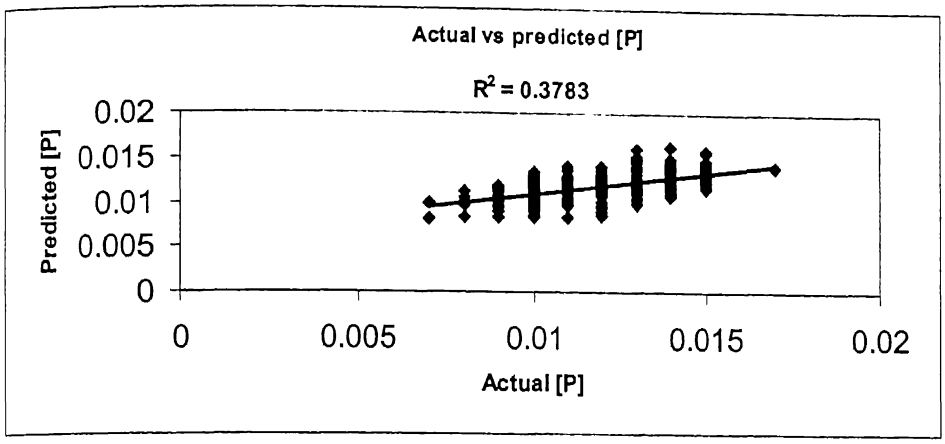

Fig 4.27 Comparison between actual and predicted phosphorous at the end of blow by modified Healy's model for vessel-2 of case study-2 (Eq. 4.14)

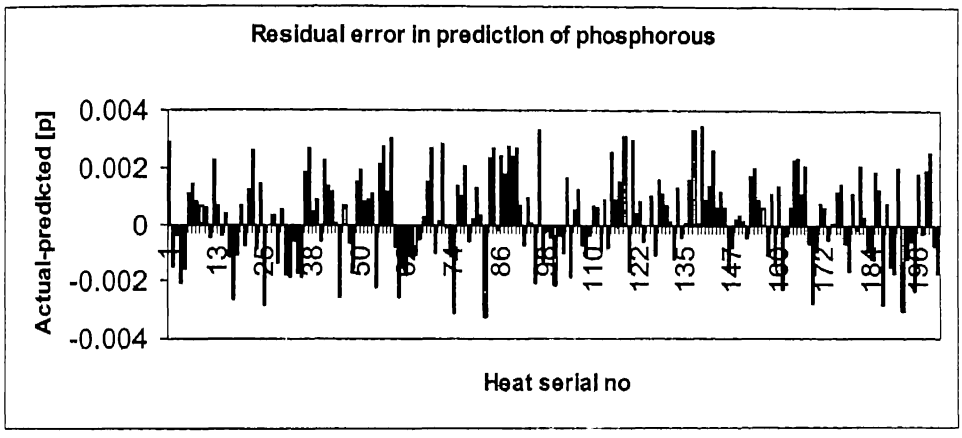

Fig4.28 Residual error plot for prediction of turndown phosphorous by modified Healy's model for vessel-2 of case study-2 (Eq. 4.14)

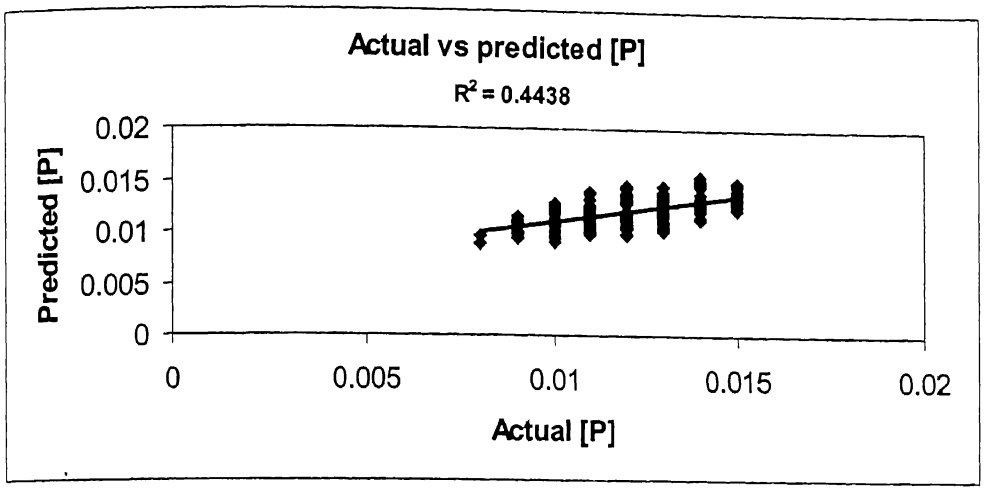

Fig 4.29 Comparison between actual and predicted phosphorous at the end of blow by modified Healy's model for vessel-3 of case study-2 (Eq. 4.15)

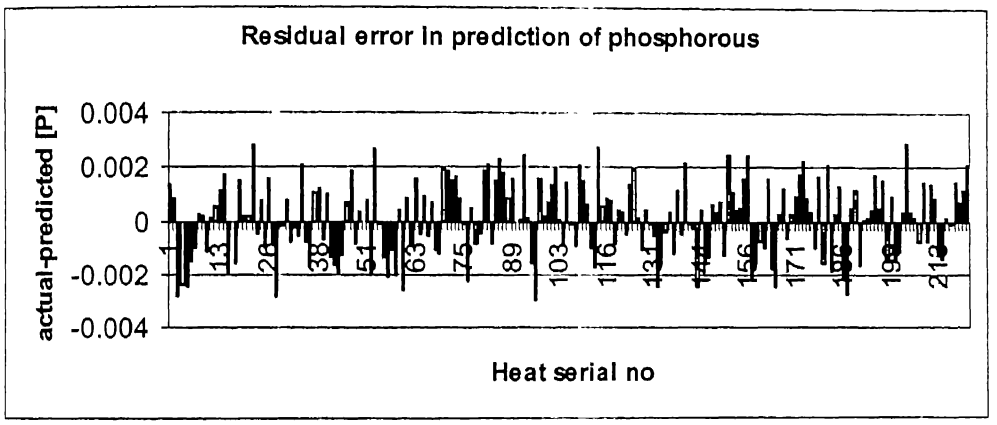

Fig 4.30 Residual error plot for prediction of turndown phosphorous by modified Healy's model for vessel-3 of case study-2 (Eq. 4.15)

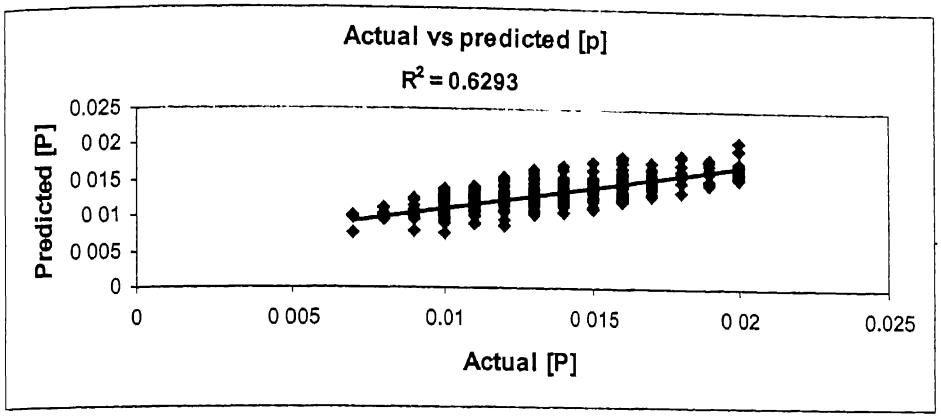

Fig 4.31 Comparison between actual and predicted phosphorous at the end of blow by modified Molecular theory model for vessel-1 of case study-2 (Eq. 4.16)

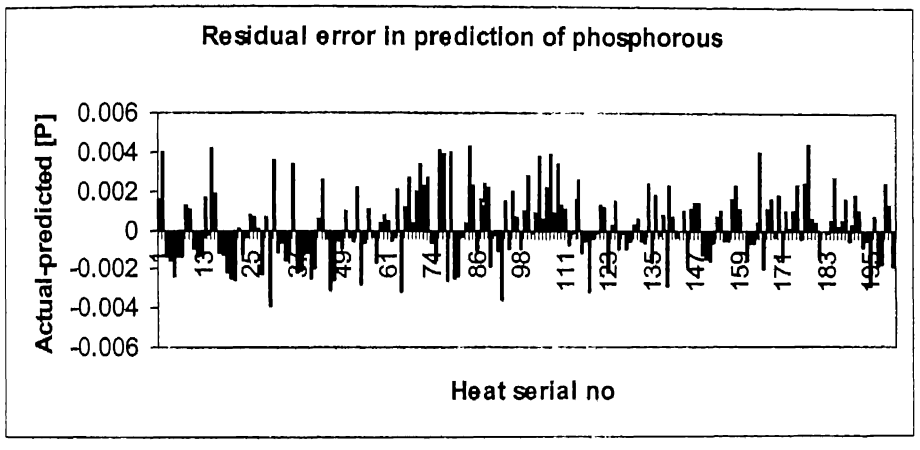

Fig 4.32 Residual error plot for prediction of turndown phosphorous by equation by modified Molecular theory model for vessel-1 of case study-2 (Eq. 4.16)

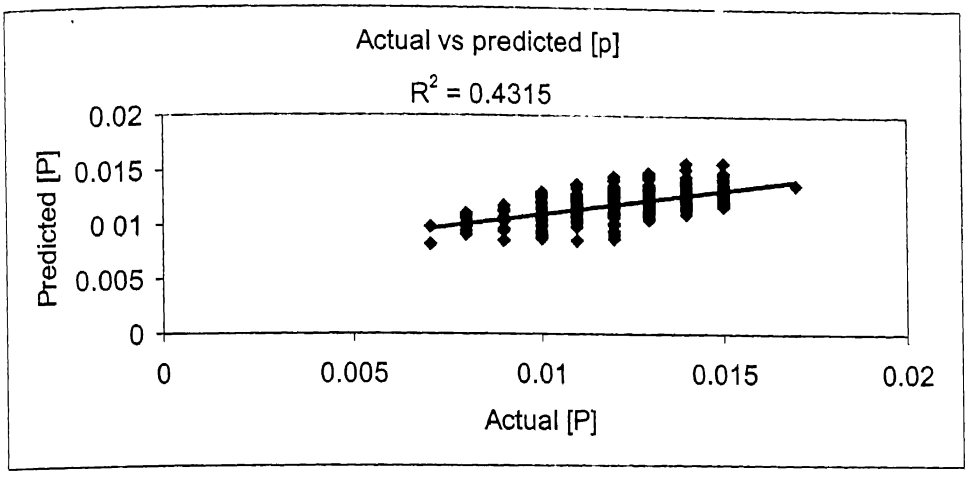

Fig 4.33 Comparison between actual and predicted phosphorous at the end of blow by modified Molecular theory model for vessel-2 of case study-2 (Eq. 4.17)

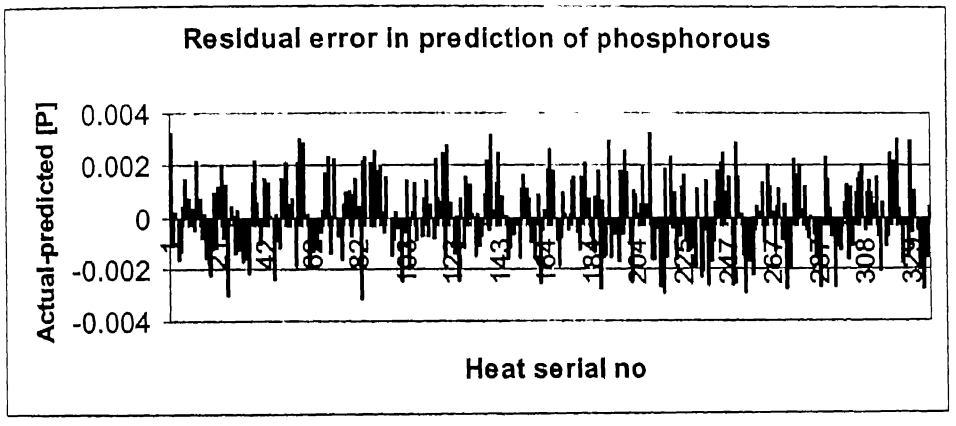

Fig 4.34 Residual error plot for prediction of turndown phosphorous by modified Molecular theory model for vessel-2 of case study-2 (Eq. 4.17)

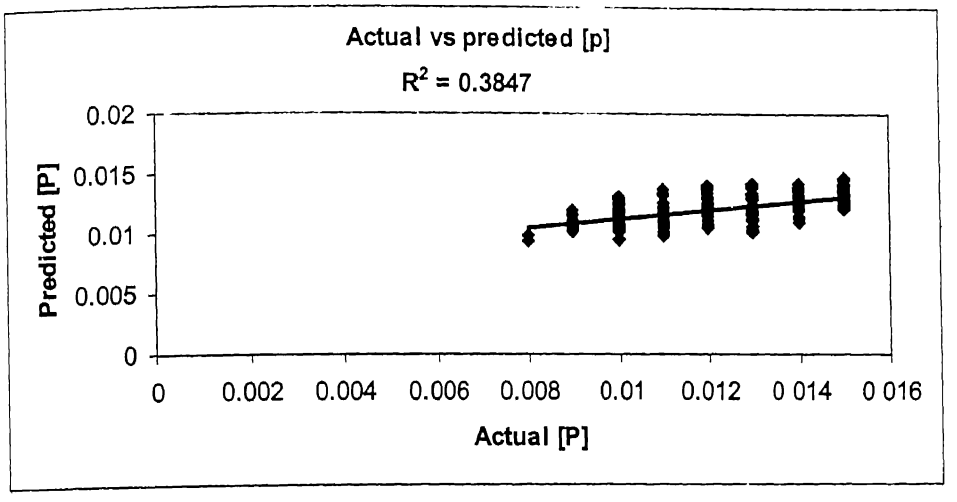

Fig 4.35 Comparison between actual and predicted phosphorous at the end of blow by modified Molecular theory model for vessel-3 of case study-2 (Eq. 4.18)

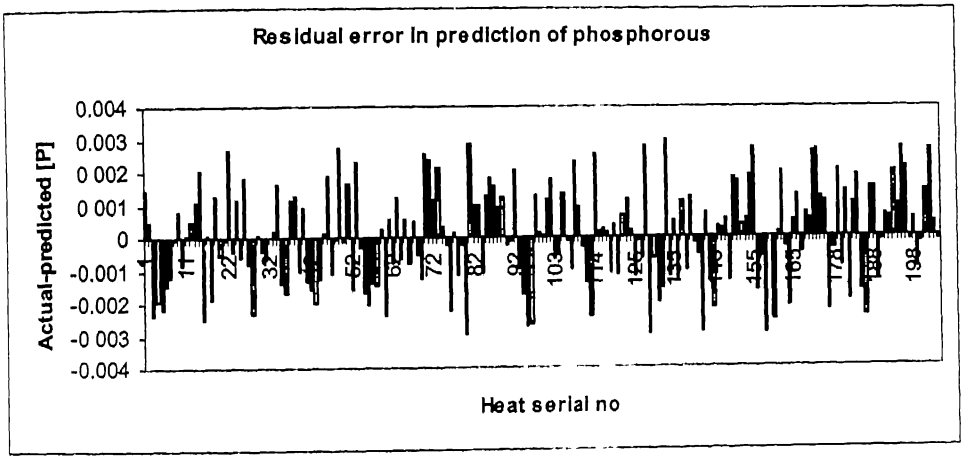

Fig 4.36 Residual error plot for prediction of turndown phosphorous by modified Molecular theory model for vessel-3 of case study-2 (Eq. 4.18)

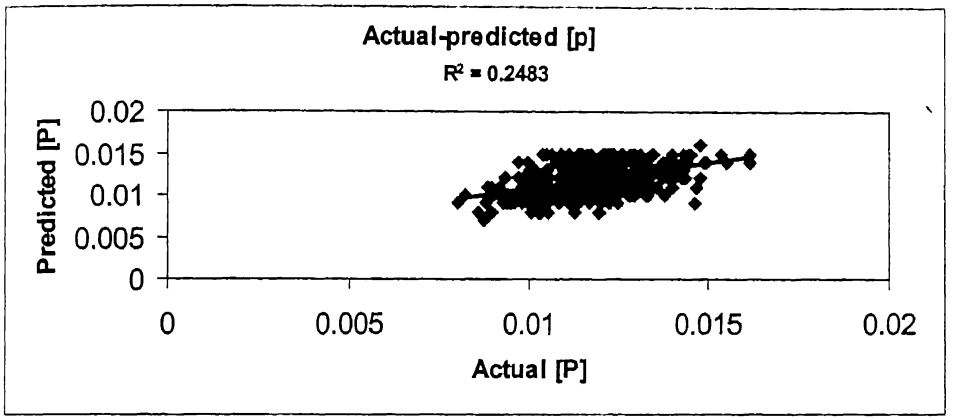

Fig 4.37 Comparison between actual and predicted phosphorous at the end of blow by modified Optical basicity model for vessel-1 of cases study-2 (Eq. 4.19)

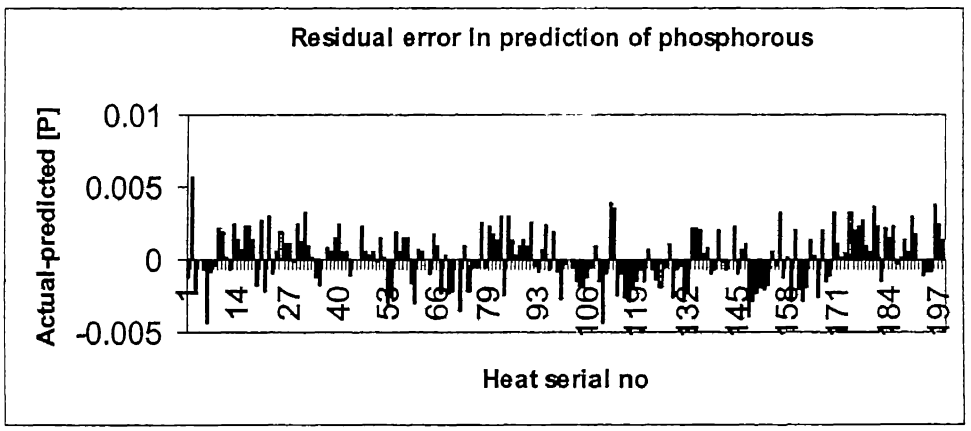

Fig 4.38 Residual error plot for prediction of turndown phosphorous by modified Optical basicity model for vessel-1 of cases study-2 (Eq. 4.19)

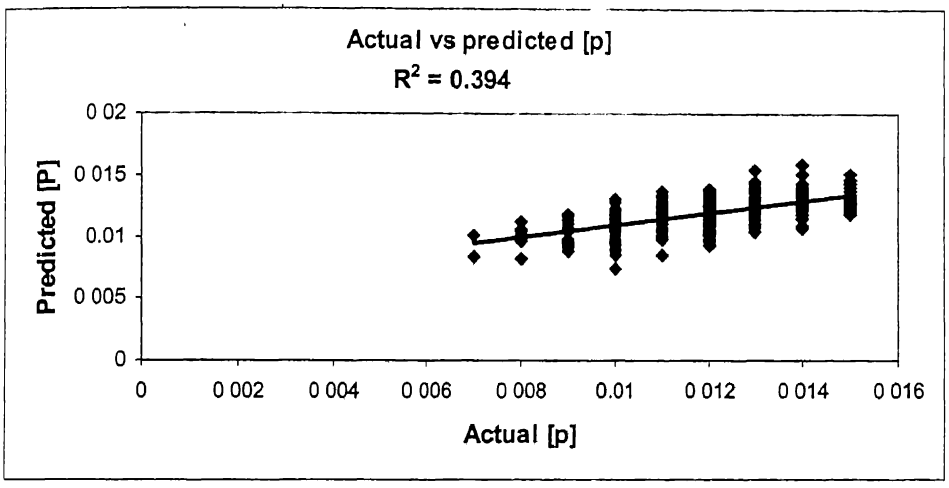

Fig 4.39 Comparison between actual and predicted phosphorous at the end of blow by modified Optical basicity model for vessel-2 of cases study-2 (Eq. 4.20)

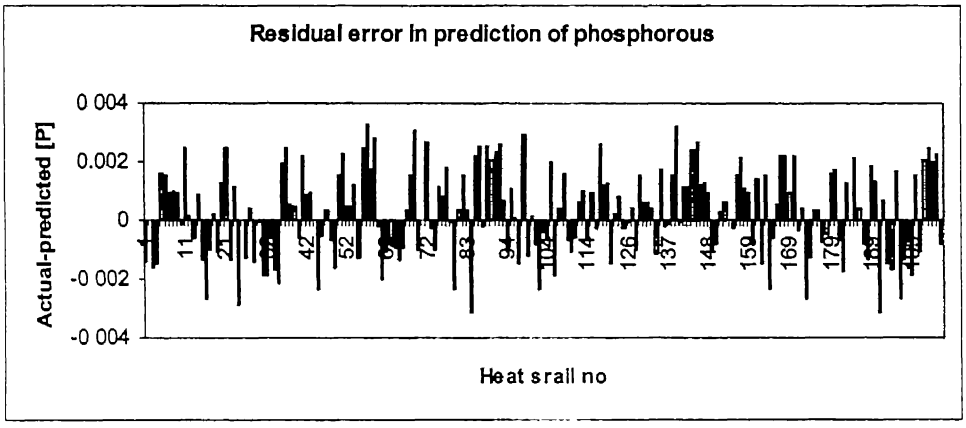

Fig 4.40 Residual error plot for prediction of turndown phosphorous by modified Optical Basicity model for vessel-2 of cases study-2 (Eq. 4.20)

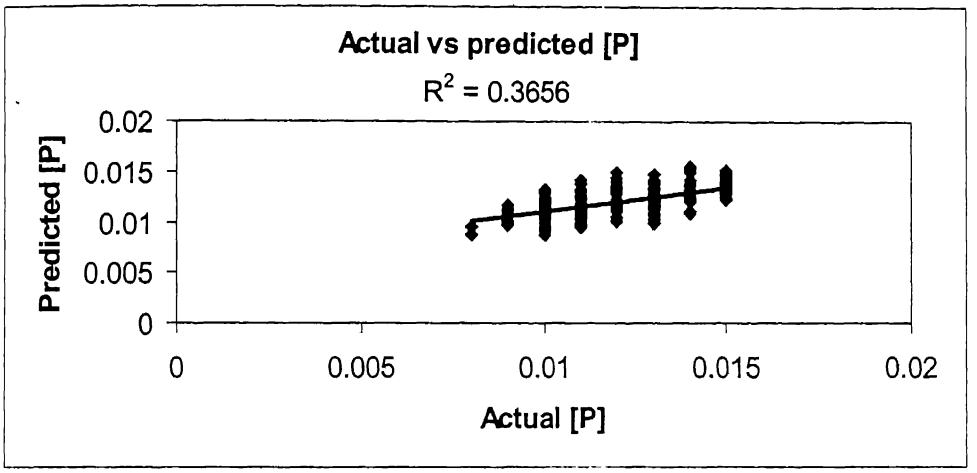

Fig 4.41 Comparison between actual and predicted phosphorous at the end of blow by modified Optical basicity model for vessel-3 of cases study-2 (Eq. 4.21)

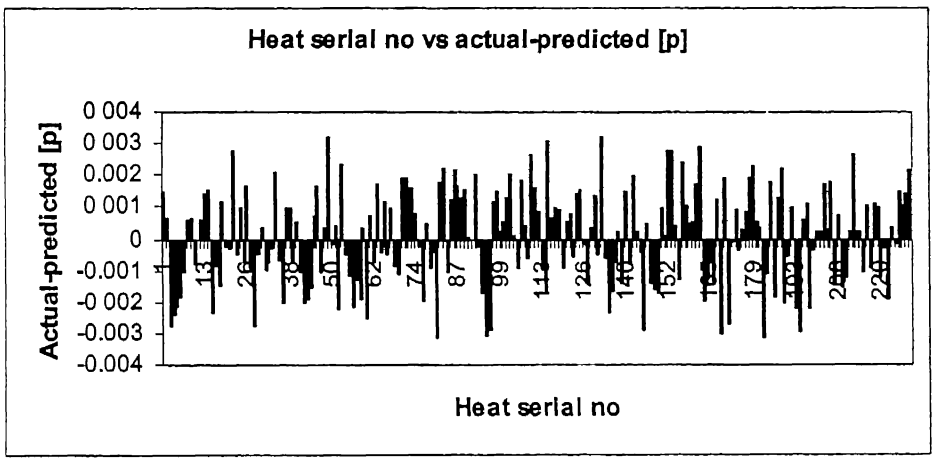

Fig 4.42 Residual error plot for prediction of turndown phosphorous by modified Optical basicity model for vessel-3 of cases study-2 (Eq. 4.21)

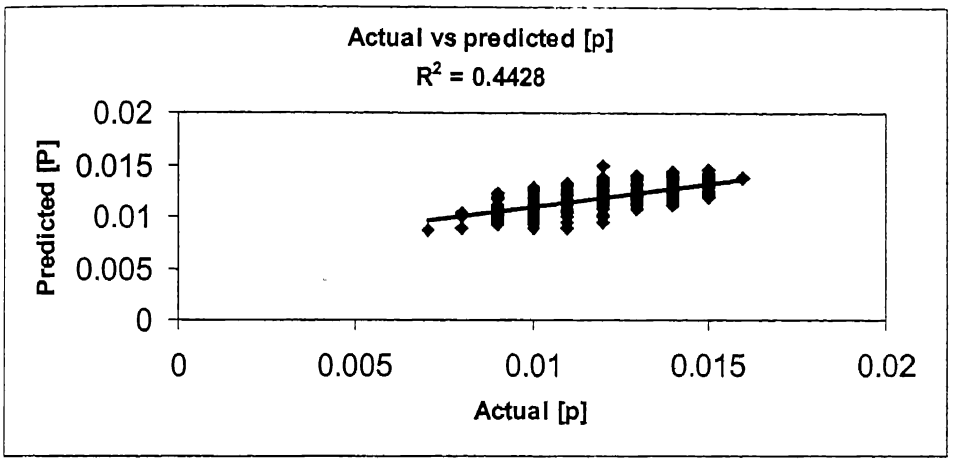

Fig 4.43 Comparison between actual and predicted phosphorous at the end of blow by modified quadratic formalism model for vessel-1 of case study-2 (Eq. 4.22)

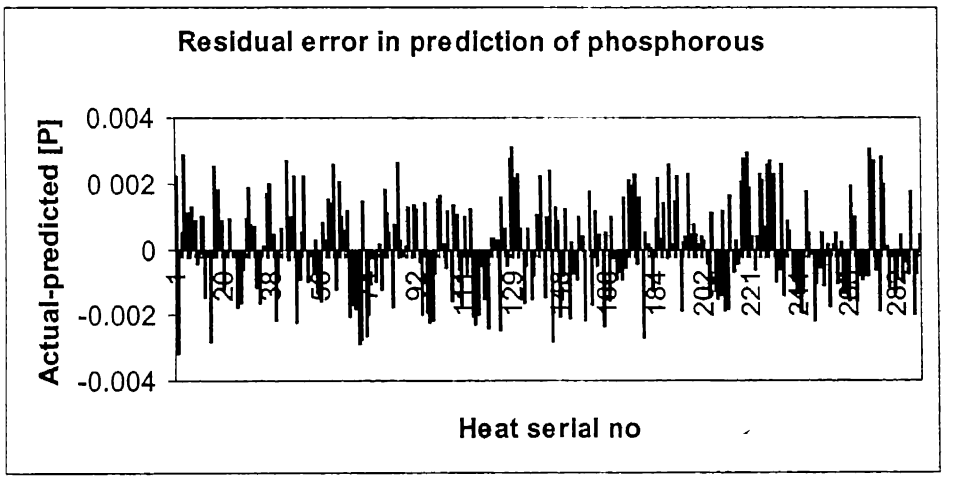

Fig 4.44 Residual error plot for prediction of turndown phosphorous by modified quadratic formalism model for vessel-1 of case study-2 (Eq. 4.22)

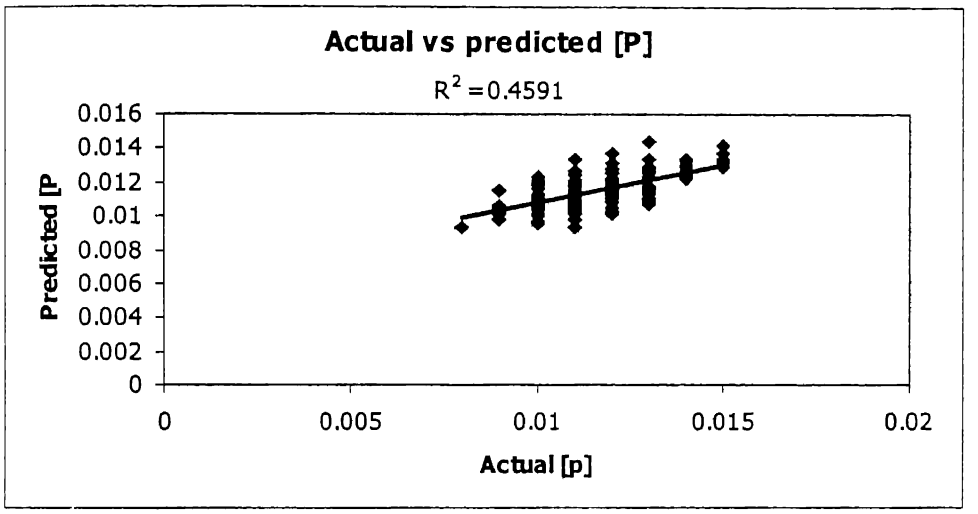

Fig 4.45 Comparison between actual and predicted phosphorous at the end of blow by modified quadratic formalism model for vessel-2 of case study-2 (Eq. 4.23)

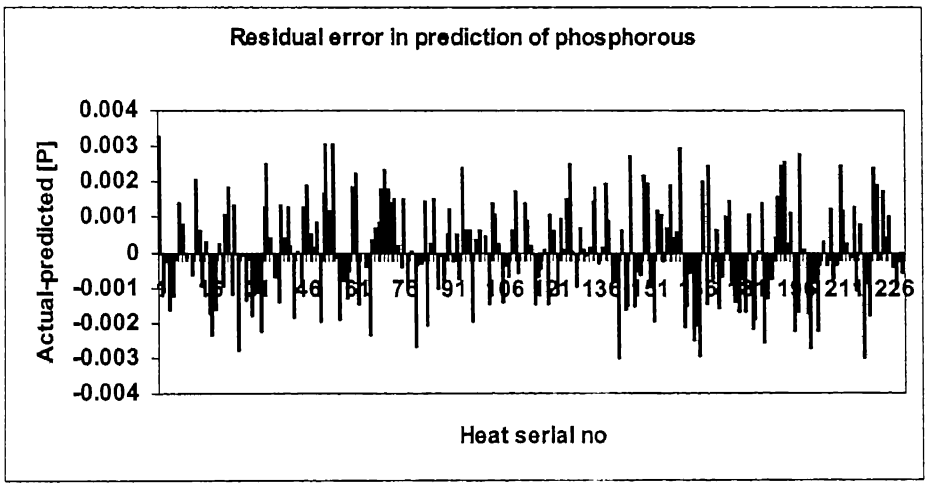

Fig 4.46 Residual error plot for prediction of turndown phosphorous by modified quadratic formalism model for vessel-1 of case study-2 (Eq. 4.23)

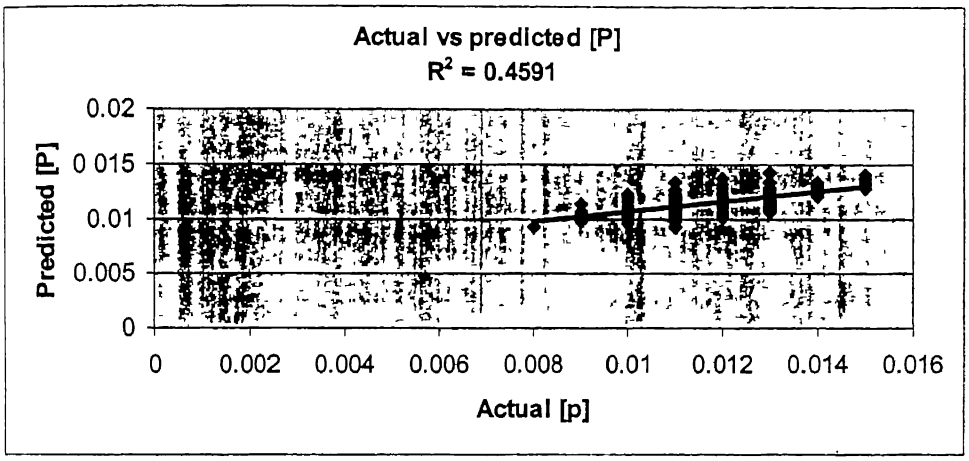

Fig 4.47 Comparison between actual and predicted phosphorous at the end of blow by modified quadratic formalism model for vessel-3 of case study-2 (Eq. 4.24)

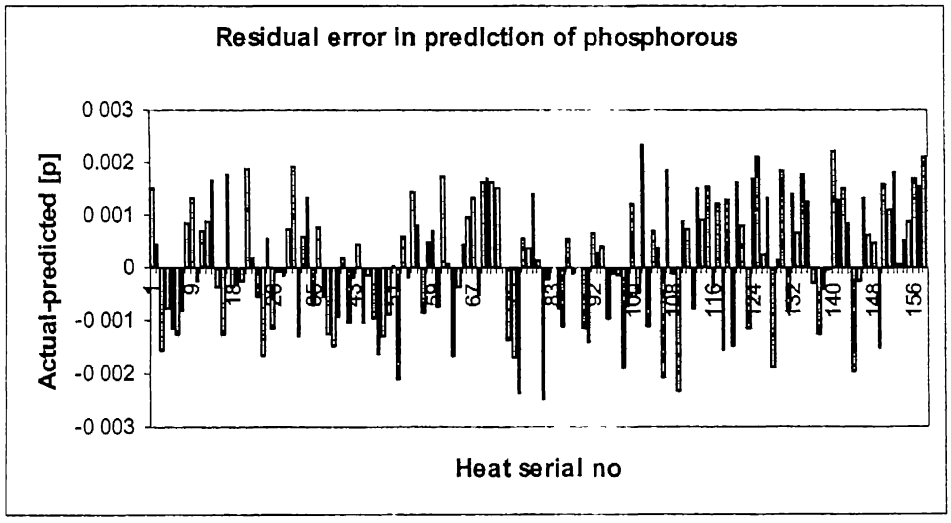

Fig 4.48 Residual error plot for prediction of turndown phosphorous by modified Quadratic formalism model for vessel-3 of case study-2(Eq. 4.24)

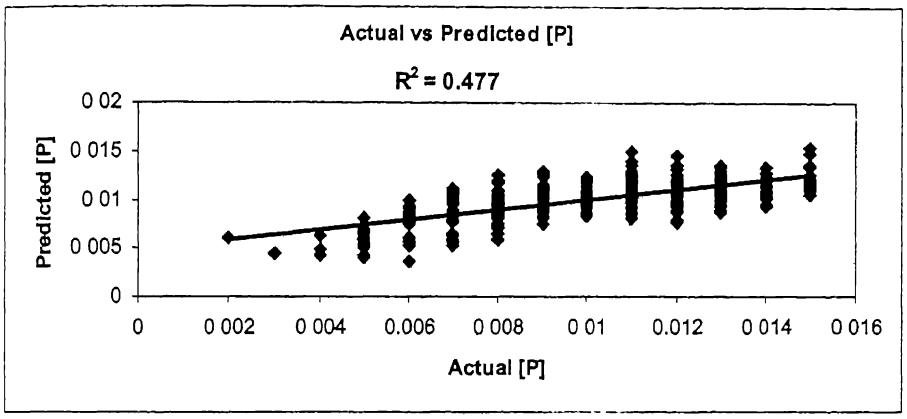

Fig 4.49 Comparison between actual and predicted phosphorous at the end of blow by modified Molecular theory model for set-1 of case study-3 (Eq. 4.25)

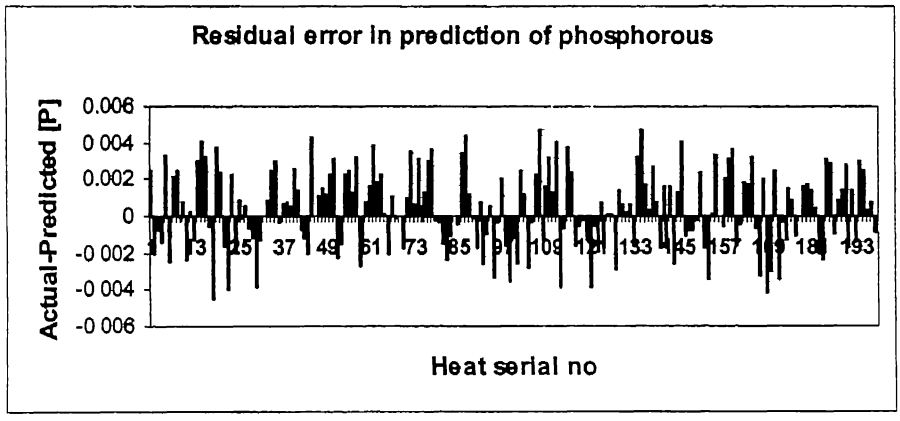

Fig 4.50 Residual error plot for prediction of turndown phosphorous by modified Molecular theory model for set-1 of case study-3 (Eq. 4 .25)

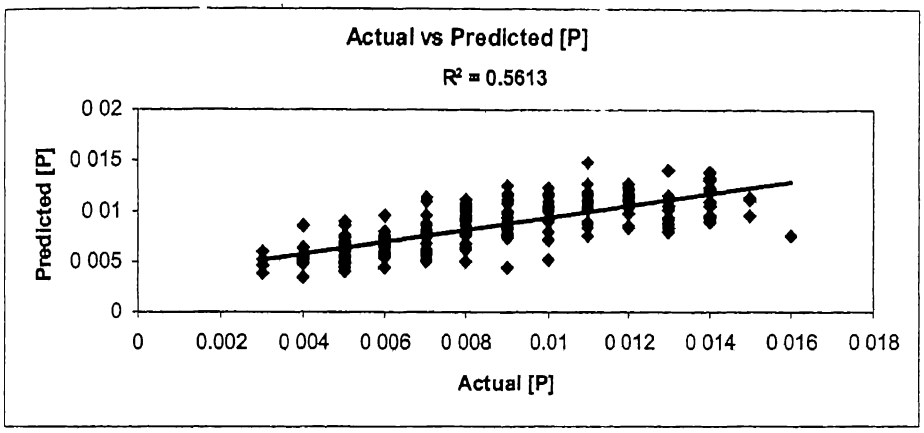

Fig 4.53 Comparison between actual and predicted phosphorous at the end of blow by modified Molecular theory model for set-3 of case study-3 (Eq. 4.27)

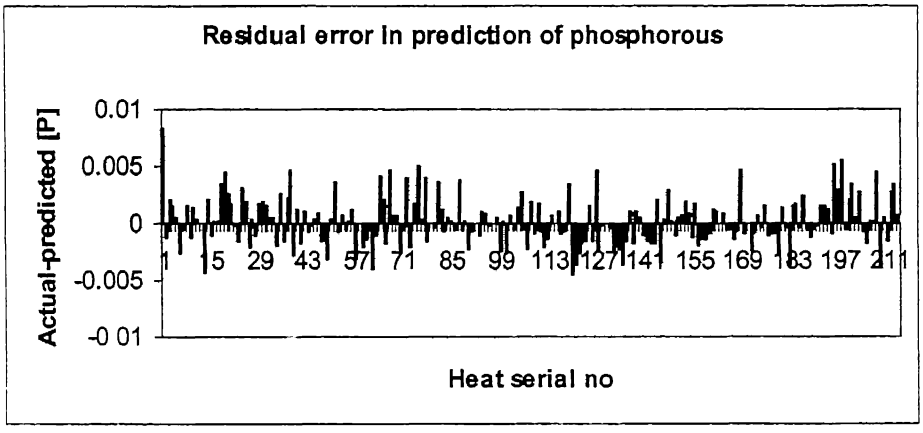

Fig- 4.54 Residual error plot for prediction of turndown phosphorous by modified Molecular theory model for set-3 of case study-3 (Eq. 4.27)

Chapter 5

Effect of MgO and Al_2O_3 on slag morphology and phosphorous distribution

5.0 Introduction

In this chapter the results of microstructural investigations on different types of slags are discussed so as to understand the effect of MgO and Al_2O_3 on slag morphology and phosphorous distribution. Attention is focused specially on the proportion of solid and liquid slag and the distribution of phosphorous in different phases, specially the phosphorous content of di-calcium silicate under different conditions. The molecular slag model, described in chapter-2, is applied to the collected data. The details of slags formed at four different plants are summarized in Table 5.1, along with the respective operating practices.

5.1 Morphology of slag with different MgO and Al_2O_3 contents

The typical microstructures of low MgO slag, high MgO slag, low Al_2O_3 slag and high Al_2O_3 slags are shown in Fig 5.1-5.6.

(a) Microstructures in Fig 5.1 and 5.2 pertain to the slag containing (~8 %) MgO with basicity ~3.4, hot metal contains low phosphorous (<0.07), and tapping temperature is ~1670^{0}C.

The X-Ray diffraction analysis shows that the mineral phases present in the sample are $2CaO.Fe_2O_3$, $2CaO.SiO_2$ and Ca-Fe-Al ferrite. The SEM/EPMA analysis shows that the major phases present in the sample are C_2S (the gray grains marked as 1), wustite solid solution (marked as 2) and $2CaO.Fe_2O_3$/ calcium aluminium ferrite (marked as 3). EPMA shows that the phosphorous content in the C_2S may vary from 4.5-6% depending upon the size of the grains. The large C_2S grains contain 5-6% phosphorous and the smaller grains contain 4-5% phosphorous. Whether this phosphorous is present as dissolved phosphorous or as fractions of $Ca_5(PO_4)_2(SiO_4)_6$ is yet to be determined Almost no phosphorous is observed in wustite solid solution There is no evidence of tri-calcium silicate (C_3S) is seen in the sample. (Fig 5.1-Fig 5.2).

Table-5.1 Details slag composition collected from different steel plants

Plant	Converter specification and type of slag		Bulk slag composition (average)	Microstructure
1	High MgO (8%) slag and low phosphorous hot metal (<0.07%) (Bottom stirring, 300 ton converter)		CaO (42%), MgO (8 %) FeO (22 %), Al_2O_3 (1.4%), Basicity 3.4	Fig-5.1- Fig 5.2
2	Low MgO (0.9 %) slag and high phosphorous (0.2-0.26) hot metal (Bottom stirring, 140 ton converter)		CaO (53%), MgO (0.9%), FeO (24 %), Al_2O_3 (0.9), Basicity 3.9	Fig-5.3
3	High MgO (7%) and low Al_2O_3 (1%) slag and medium phosphorous (0.15%) hot metal (No bottom stirring, 140 ton converter)		FeO (20 %), MgO (7.%), Al_2O_3 (1%) Basicity 3.4	Fig-5.4
4	300 ton with bottom stirring	Case-B (High MgO (10 %), low Al_2O_3 (<2%)slag high phosphorous (0.2%) hot metal)	CaO (47 %), FeO (18 %), MgO (10 %), Al_2O_3 (2%) Basicity 3	Fig-5.5
		Case-A (High MgO (10 %) and high Al_2O_3(4%) in slag and high phosphorous (0.2%) hot metal	CaO (47 %), FeO (18 %), MgO (10 %), Al_2O_3 (4 %) Basicity 3	Fig-5.6

(b) Microstructure in Fig 5.3 is obtained for low MgO (~0.9 % MgO) when hot metal contain high phosphorous (0.2-0.26%), and slag basicity is ~ 3.5 at tapping temperature of ~1700^{0}C

The SEM/EPMA analysis of a slag sample shows that the gray grains (marked as 1) are C_2S (approximate composition), and the white grains (marked as 2) are wustite solid solution and small dark (black) grains (marked as 3 in the micrograph) are $2CaO.Fe_2O_3$ / $CaO.Fe_2O_3$/calcium-aluminium-ferrite.

A typical spot analysis of C_2S grains and wustite solid solution is as follows:

Table-5.2 Results of spot analysis for high phosphorous hot metal high MgO slag

Phase	Mg	Al	Si	P	S	Ca	Ti	Mn	Fe
Ca-Fe-Al (Point-3 in Fig-5.3)	0.00	1.74	0.78	0.20	0.31	42.01	5.28	0.55	49.12
Wustite solid solution (Point-2 in Fig-5.3)	3.04	0.09	0.28	0.32	0.58	5.55	0.00	4.90	85.24
C_2S (Point-1 in Fig-5.3)	0.00	0.17	15.69	4.76	0.52	70.21	1.03	.030	7.33
C_2S (Point-4 in Fig-5.3)	0.00	0.21	17.47	4.55	0.47	71.73	1.18	0.21	4.17

Dicalcium silicate contains (4.5-4.75%) phosphorous where as wustite solid solution contains only (0.08-0.2%) phosphorous or the ratio of phosphorous in the C_2S to phosphorous in the wustite solid solution is of the order of 24:1. Content of MgO varies from place to place, at some location MgO is as much as 3%, at other places it is absent. No tri-calcium silicate (C_3S) is seen in the sample (Fig-3).

(c) Microstructure in Fig 5.4 is obtained for high MgO (9-11%) slag when the phosphorous content of hot metal is (0.07-0.15%P) and slag basicity is 3.5 at 1660^{0}C

The EPMA analysis of the slag sample shows that the grains (marked as 1) are C_2S and the white grains (marked as 2) are wustite solid solution. Ratio of MgO in the wustite solid solution to the MgO inC_2S is approximately 2:1. Ratio of phosphorous in the C_2S to the phosphorous in the wustite solid solution is of the order of 17:1.

(d) Microstructure in Fig 5.5 and Fig 5.6 is obtained for high MgO (~9-11%) and low Al_2O_3 (<2%) high Al_2O_3 (~4%) slag respectively when the phosphorous content of hot metal is (0.15-0.2%P) and slag basicity is ~3.2 at ~1680^{0}C.

Optical microstructure of low Al_2O_3 (Fig-5.5) slag sample shows a higher volume fraction C_2S (point-2) and lesser amount of calcium-aluminium-ferrite (point-3), compared to the high Al_2O_3 (compare with Fig 5.6) slag.

5.1.1 Discussion

The following general observations can be made on the basis of optical micrograph, SEM, EPMA and X-Ray diffraction investigations regarding the effects of MgO and Al_2O_3, tapping temperature and basicity on phosphorous distribution and size of the C_2S grains:

(i) C_2S is stabilized by higher basicity, lower temperature and higher phosphorous content of hot metal.

(ii) The presence of MgO decreases the size of the C_2S grains as well as the phosphorous content of C_2S.

(iii) The presence of Al_2O_3 stabilizes calcium-aluminium–ferrite and reduces both the amount and the crystal size of C_2S and also its phosphorous content.

According to the ionic theory of slag, in a slag containing more than 7 wt% MgO, content, primarily the Mg containing wustite tends to become solid. Wustite is first

precipitated and the fluid slag becomes depleted in mobile cations before the PO_4^{3-} binding dicalcium silicate is formed. Due to this, both the amount of C_2S and the phosphorous of C_2S content are reduced. Thus, dephosphorization is hindered.

In converter slags with higher alumina contents (>2%), the aluminium-binding anion complexes, together with $Fe2O_5^{4-}$ and Ca^{2+}, will initially form calcium-aluminium ferrite on solidification. No PO_4^{3-} anion complexes will be incorporated in its crystallites. The formation of dicalcium silicate is also hindered because C_2S forms at the early stages of the blow but at that time calcium aluminium ferrite forms preferentially due to the presence of Al_2O_3. If aluminium is present as AlO_4^{5-} anion complex in fluid converter slag, the tetrahedrons SiO_4^{4-}, AlO_4^{5-}, PO_4^{3-}, form simple chains by polymerization. Here, a partial substitution of SiO_4^{4-} by AlO_4^{5-} or PO_4^{3-} may occur as a result of ion isomorphism. On solidification, the tetrahedrons of AlO_4^{5-} and PO_4^{3-} are incorporated in the crystallites of dicalcium silicate by partial substitution of SiO_4^{4-} ions. Addition of bauxite to converter slags causes a surplus of AlO_4^{5-} anion complexes and if neutralization is taken into consideration the incorporation of PO_4^{3} anion complexes in the formation of dicalcium silicate crystallites is suppressed. Thus, in the presence of Al_2O_3 in the slag dephosphorization is hindered.

5.2 Effect of incorporation of C_2S as a parameter in the molecular theory model.

It has been practically observed that in the case of high phosphorous hot metal the percentage P_2O_5 dissolved in dicalcium silicate is several times (2-6 times) more than the P_2O_5 dissolved in liquid slag. The formation and dissolution of dicalcium silicate is, therefore, an important parameter for the control of dephosphorization. In this section, the percentage dicalcium silicate is calculated for an overall slag composition and then incorporated as a parameter in the regression analysis. The method of calculation of the fraction of dicalcium silicate in bulk is explained in Appendix-B.

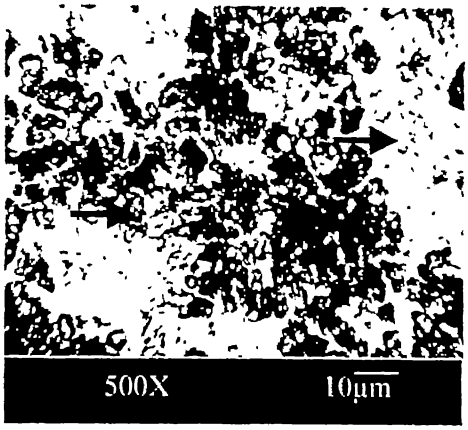

Fig-5.1 Optical micrograph of (low phosphorous (<0.07 %) hot metal) high MgO slag (8 %). Basicity 3.4. Tapping temperature 1670^{0}C (Plant-3).
Point-1 Dicalcium silicate
Point-2 Wustite solid solution

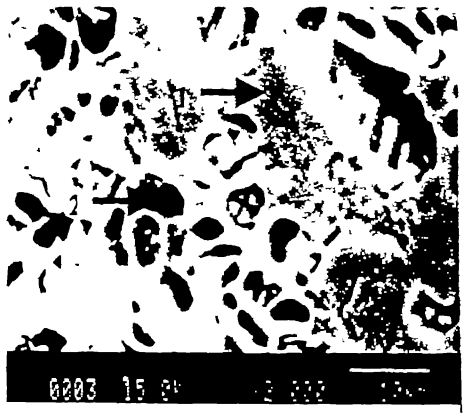

Fig-5.2 SEM micrograph of (low phosphorous (<0.07 %) hot metal) high MgO slag (8 %). Basicity 3.4. Tapping temperature 1670^{0}C (Plant-3), sample is carbon coated.
Point-1 Dicalcium silicate
Point-2 Wustite solid solution

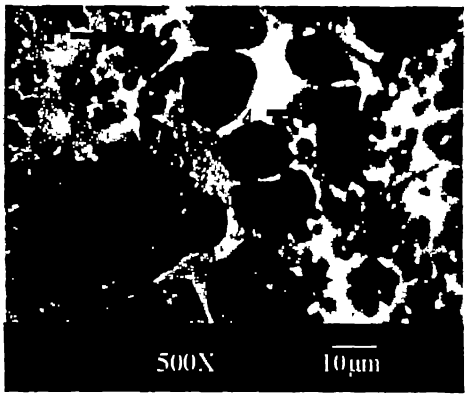

Fig-5.3 Optical micrograph of (high phosphorous (0.2%) hot metal) low (0.9 %) MgO slag. Basicity 3.9. Tapping temperature 1700^{0}C (Plant-2).
Point-1 Dicalcium silicate
Point-2 Wustite solid solution
Point-3 Calcium aluminium ferrite
Point-4 Dicalcium silicate

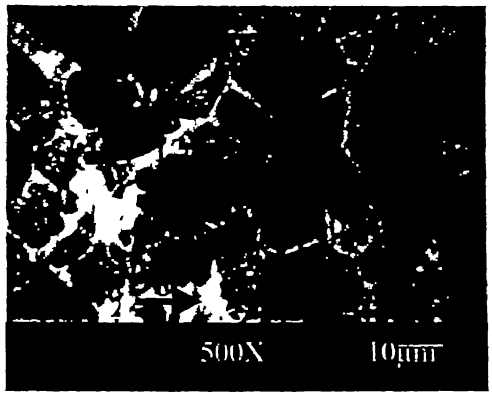

Fig-5.4 Optical micrograph of (medium phosphorous (0.15%) hot metal) high MgO (7.5%) low Al_2O_3 (1%) slag. Basicity-3.4. Tapping temperature 1660^{0}C (Plant-3).
Point-1 Dicalcium silicate
Point-2 Wustite solid solution
Point-3 Calcium aluminium ferrite

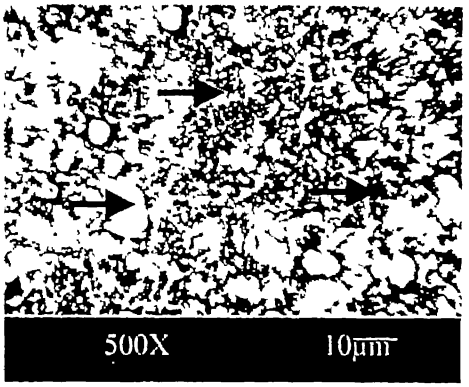

Fig-5.5 Optical micrograph of (high phosphorous (0.15-0.2%) hot metal) high MgO (10 %) and low Al_2O_3 (<2%) slag. Basicity 3. Tapping temperature 1680^0C (Plant-4 case-B).

Point-1 Dicalcium silicate
Point-2 Wustite solid solution
Point-3 Calcium aluminium ferrite/Calcium ferrite

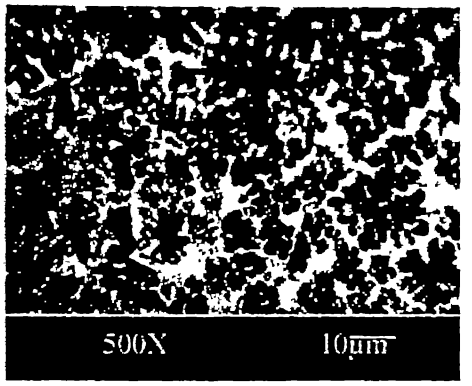

Fig-5.6 Optical micrograph of (high phosphorous (0.15-0.2%) hot metal) high MgO (10 %) high Al_2O_3 (4%) slag. Basicity 3. Tapping temperature 1680^0C (Plant-4 case-A)

Point-1 Dicalcium silicate
Point-2 Wustite solid solution
Point-3 Calcium aluminium ferrite/ Calcium ferrite

The basicity of liquid slag is calculated from the liquid slag composition (For calculation of liquid slag composition reference may be made to appendix-C). But the calculated basicity shows a high value compared to the bulk slag basicity ranging from 3.6 to 5.7. This is because when C_2S is formed SiO_2 is consumed to form C_2S and the percentage SiO_2 in liquid slag decreases, thus, the basicity in the liquid phase, defined as $\%CaO/SiO_2$, increases.

Case-A: Effect of C_2S on the phosphorous partition

In this section percent dicalcium silicate has been included as another parameter in the original molecular theory model to examine the effect of dicalcium silicate on phosphorous partition coefficient.

The following equations are obtained (Table5.3) for different selected sets of data in case study-1,2 and 3, when MLR is carried out by incorporating additional variables C_2, SVO, Ore, Hl_2, HTR and also C_2S into the original molecular theory model:

Table-5.3 Summary of models developed when C_2S is included as another parameter in the original molecular theory model for case study-4 (Case-A)

Data set	Equation	R	σ	Equation no
Set-1 of case study-1	$\log\frac{(P)}{[P]^2}=\frac{33665.2}{(T_2-255.22)}+0.0044\times HL_2-23.01\times C_2$ $+5\,8\times\log(CaO)+1.58\times10^{-5}\times SVO+0\,0002\times Ore-26.87$;S is not selected as a separate parameter	0.8	0.0026	5.1
Set-1 of case study-3	$\log\frac{(P)}{[P]^2}=\frac{321524.3}{[T_2-255.22]}+2.68\times C_2+0\,65\times\log(CaO)-365.7$ C_2S is not selected as a separate parameter	0.75	0.0026	5.2

For more details regarding 't' values reference may be made to Table 5.6.

It is seen from Table 5.3 that C_2S is not selected as an additional parameter in regression equation but correlation coefficient improves , compare Eq. 4.4 (R is 0.47) with Eq. 5.1 (R is 0.8) , Eq. 4.25 (R is 0 69) with Eq 5.2 (R is 0.75).

Case-B: Distribution of P_2O_5 in C_2S and in liquid slag

It is observed that the percentage of P_2O_5 in dicalcium silicate may vary from 2-8% depending upon the phosphorous content of hot metal. Thus, the ratio of P_2O_5 in solid slag (C_2S) and liquid slag may change depending upon specially the phosphorous content of hot metal. In this section, the ratio of P_2O_5 in solid slag and liquid slag is assumed a priori as 1, 2, and 3 and then regression is done to find which ratio gives the best results. In order to predict the phosphorous content of metal, it is necessary to do mass balance for slag and metal phase. The procedure adopted is explained in appendix C.

The following equations are obtained, (Table5.4) when MLR is carried out by incorporating the additional parameters C_2, SVO, Ore, Basicity, HTR and also C_2S in the original molecular theory model, for different distribution ratios of phosphorous in C_2S and in liquid part of slag.

Table-5.4 Comparison of Models developed with and without C_2S as a parameter in the original molecular theory model for case study-4, (Case-B).

Data set	Ratio of P_2O_5 in C_2S in liquid slag	Equation	R	σ	Equation no.
Vessel-1 of case study-2	1	$\log\frac{(P)}{[P]^2}=\frac{8111.37}{(T_2-255.22)}+0.13\times basicity$ $+Ore\times 0\ 017+0.079\times C_2S-1.74$ C_2S is selected as an additional parameter	0.71	0.0017	5.3
	2	$\log\frac{(P)}{[P]^2}=\frac{7404.16}{(T_2-255.22)}+2\ 72\times Basicity$ $+0.017\times Ore+2.97\times C_2-1.03$ C_2S is not selected as an additional parameter	0.73	0.0016	5.4

Table-5.4 continued...

Comparison of Models developed with and without C_2S as a parameter in the original molecular theory model for case study-4, (Case-B).

Data set	Ratio of P_2O_5 in C_2S in liquid slag	Equation	R	σ	Equation no.
Vessel-1 of case study-2	3	$\log\frac{(P)}{[p]^2} = \frac{9252.81}{(T_2 255.22)} + 0.04 \times basicity$ $+0.011 \times Ore + 1.37 \times \log(CaO) - 3.39$ C_2S is not selected as an additional parameter	0.73	0.0016	5.5
Vessel-1 of case study-2	Only percent C_2S in slag as a parameter	$\log\frac{(P)}{[P]} = 12441.46 \times \frac{1}{(T_c - 255.22)}$ $+1\ 56 \times C_2 + 0.97 \times \log(CaO) + 0.0061 \times SVO$ $+0\ 12 \times Basicity + 0.018 \times Ore - 5.78$ C_2S is not selected as an additional parameter	0.68	0.0024	5.6

For more details regarding individual 't' values of different parameters reference may be made to Table 5.7.

In the equations 5.3, 5.4 and 5.5 regression is done considering the ratio of P_2O_5 in C_2S and in liquid slag 1, 2 and 3, respectively. Percent C_2S is selected as a significant parameter only in the Eq. 5.3, where the correlation coefficient is 0.71. With increasing the ratio of P_2O_5 in C_2S and in liquid slag, correlation coefficient increases to 0.73 in Eq. 5.4 and 5 5. In Eq.5.5 a better correlation coefficient (0.78) is obtained if T_2 is taken as a parameter instead of $\frac{1}{(T_2 - 255.22)}$, but for the sake of similarity with the other equations

we have taken $\frac{1}{(T_2 - 255.22)}$ as a parameter. The variation of correlation coefficient (R) with different ratios of P_2O_5 in C_2S and in liquid slag is shown in Fig 5.7. In Eq. 5.6 when only C_2S is included as a parameter without considering the distribution of P_2O_5 in C_2S and in the wustite solid solution we get a poor correlation coefficient (0.68). So the distribution of P_2O_5 in the different phases is important. According to Fig 5.7 best results are obtained when the ratio of P_2O_5 in C_2S and wustite solid solution phase is assumed a priori as approximately 5.

The sign of different variables in the regression equations for Case-A and Case-B of case study-4 are listed in Table-5.4. The signs of all selected variables are positive except for the case of carobn in set1 of case study 1. It may how ever be noted that Hl_2 is selected as a variable. Most significant variables are temperature, log(CaO), C_2, basicity and Ore.

It is surprising that when C_2S is incorporated in the model, log(Fe) is not selected as a parameter in any of the cases. This may partly be due to the variation of iron content of slag is in a small range.

Table-5.5 Sign of selected variables for molecular theory model (Case-A and B)

Case study-4	Data Set		Variables										
			$\frac{1}{(T_2 - 255.22)}$	Log (CaO)	Log (Fe)	C 2	SVO	Basi-city	C_2S	Ore	HT R	Hl_2	Ore_2
CaseA	Set-1 of case study-1		+	+		- *	+					+	+
	Vessel-1 of case study-2		+	+		+	+	+		+			
	Set-1 of casesutdy-3		+	+		+							
Case B	Vesse l 1 of case study-2	Ratio-1 of P_2O_5 in C_2S and liquid slag is 1	+					+	+	+			
		Ratio-1 of P_2O_5 in C_2S and liquid slag is 2	+			+		+		+			
		Ratio-1 of P_2O_5 in C_2S and liquid slag is 3	+			+		+		+			

Table-5.6 Summary of 't' values for significant variables of case study-4, (Case-A).

Molecular theory model including C_2S as an another parameter				Additional variable for tuning T_2, SVO, C_2, HTR, Ore, Basicity,C_2S, Hl_2		
Data set	Dependent variable	Variables selected		Variables rejected	R	σ
		Variables	(t) value for selected variables			
Set-1 of plant-1	$\log\frac{(P)}{[P]^2}$	Ore	1.86	HTR, , Ore, Log(Fe), C_2S	0.8	0.0026
		$\frac{1}{(T_2-255.22)}$	6.59			
		Hl_2	2.56			
		C_2	-5.07			
		Log(CaO)	4.38			
		SVO	2.89			
Vessel-1 of plant-2	$\log\frac{(P)}{[P]^2}$	T_2	-12.78	HTR, , Log(Fe), C_2S, $\frac{1}{(T_2-255.22)}$	0.67	0.0025
		Ore	3.77			
		Basicity	4.88			
		TDC	2.54			
		SVO	1.83			
		Log(CaO)	1.51			
Set-1 of plant-3	$\log\frac{(P)}{[P]^2}$	$\frac{1}{(T_2-255.22)}$	5.49	HTR, log(CaO), Ore SVO, log(Fe), $\frac{1}{(T_2-255.22)}$	0.75	0.0026
		C_2	3.39			
		Log(CaO)	2.39			

Table-5.7 Summary of 't' values for significant variables case study-4, (Case-B).

Molecular theory model including C_2S as an another parameter					Additional variable for tuning		
					T_2, SVO, C_2, HTR, Ore, Basicity, C2S		
Data set	Ratio of P_2O_5 in C_2S to the O in wustite solid solution	Dependent variable	Variables selected		Variables rejected	R	σ
			Variables	(t) value for selected variables			
Vessel-1 of case study 2	1	$\log\frac{(P)}{[P]^2}$	Ore	3.18	HTR, Log(Fe), log(CaO), T_2, C_2, SVO	0.73	0.0015
			$\frac{1}{(T_2-255.22)}$	4.56			
			Basicity	2.4			
			C2S	2.09			
	2	$\log\frac{(P)}{[P]^2}$	Ore	2.89	HTR, Log(Fe), log(CaO), T_2, SVO, C2S	0.73	0.0016
			$\frac{1}{(T_2-255.22)}$	3.22			
			Basicity	2.72			
			C_2	1.52			
	3	$\log\frac{(P)}{[P]^2}$	Ore	2.6	HTR, Log(Fe), log(CaO), $\frac{1}{(T_2-255.2}$, SVO, C2S	0.78	0.0016
			T_2	-4.19			
			Basicity	3.39			
			TDC	1.55			

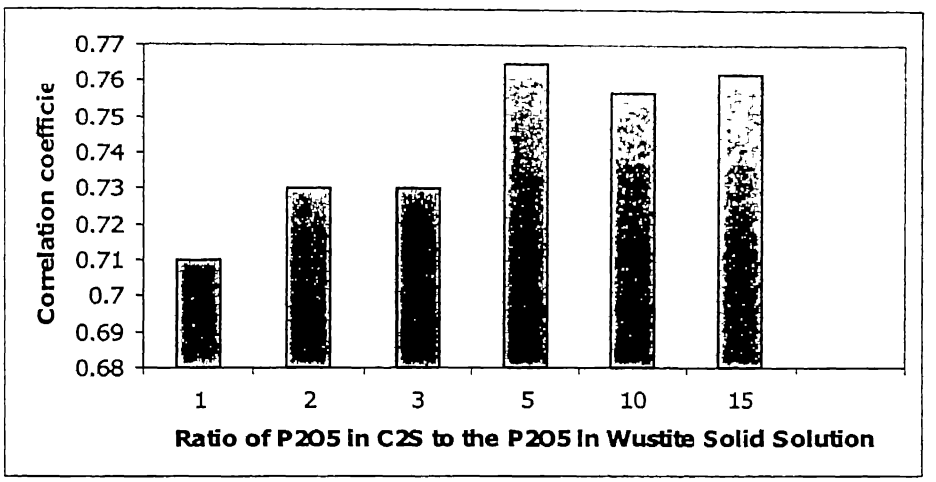

Fig-5.7 Variation of correlation coefficient with the ratio P_2O_5 in C2S and in the wustite solid solution.

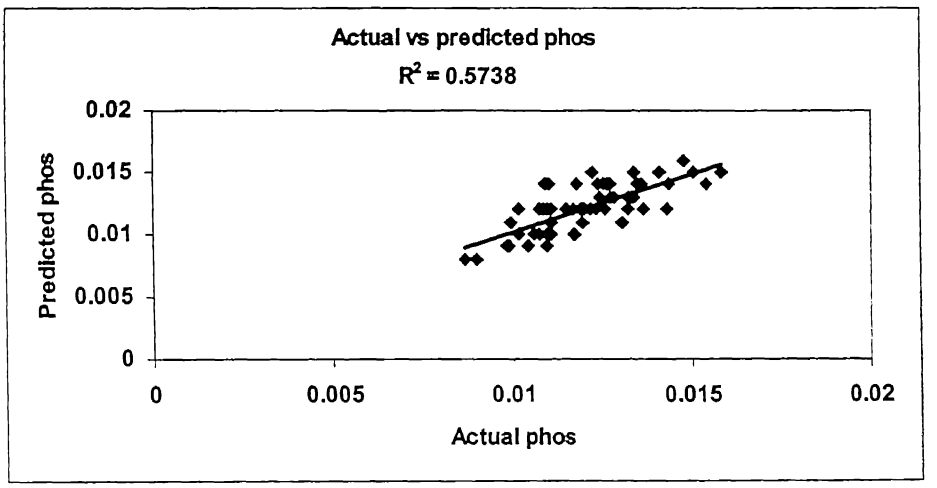

Fig 5.8 Comparison between actual and predicted phosphorous at the end of blow by modified Molecular theory model for case study-4 case-B (Eq. 5.4)

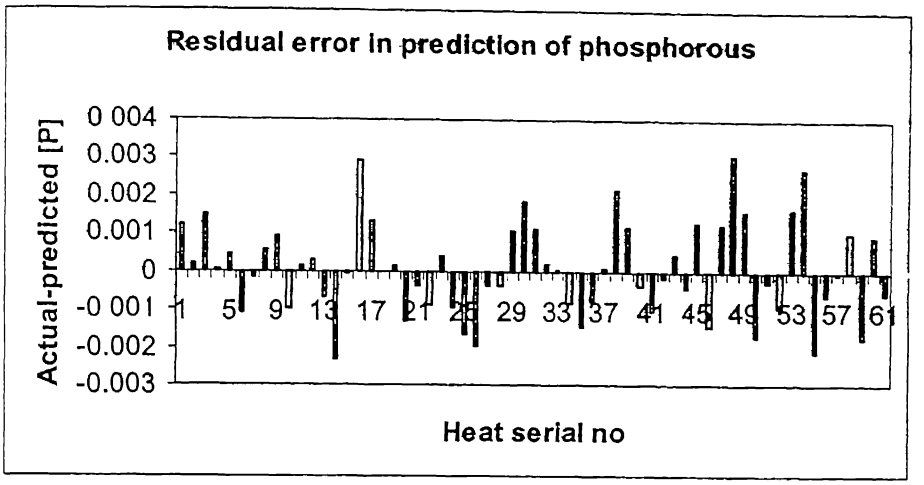

Fig 5.9 Residual error plot for prediction of turndown phosphorous by modified Molecular theory model for case study-4 case-B (Eq. 5.4)

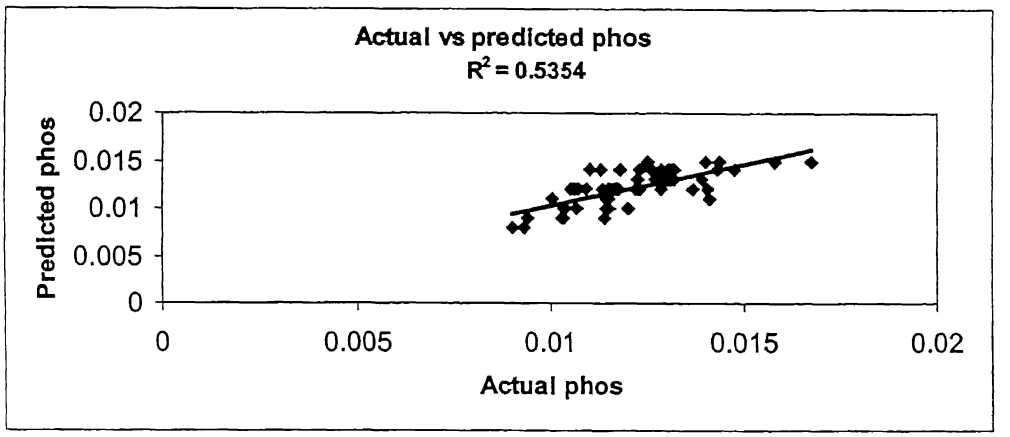

Fig 5.10 Comparison between actual and predicted phosphorous at the end of blow by modified Molecular theory model for case study-4 case-B (Eq. 5.5)

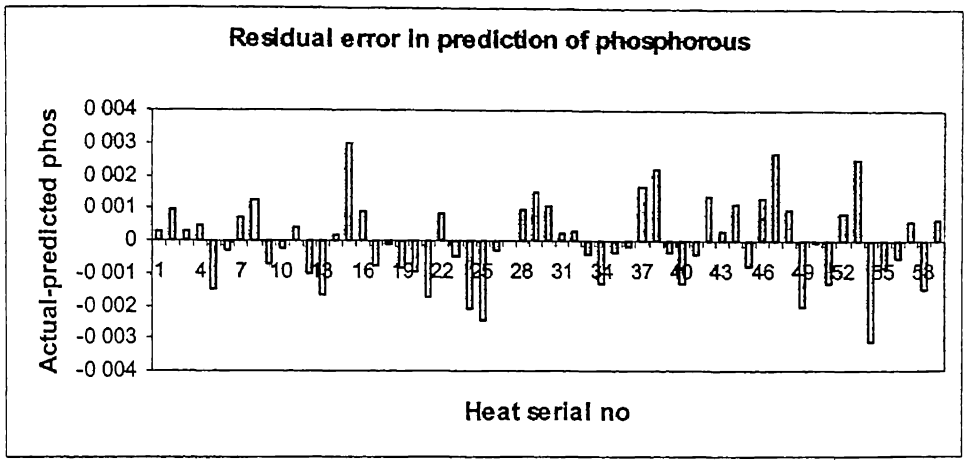

Fig 5.11 Residual error plot for prediction of turndown phosphorous by modified Molecular theory model for case study-4 case-B (Eq. 5.5)

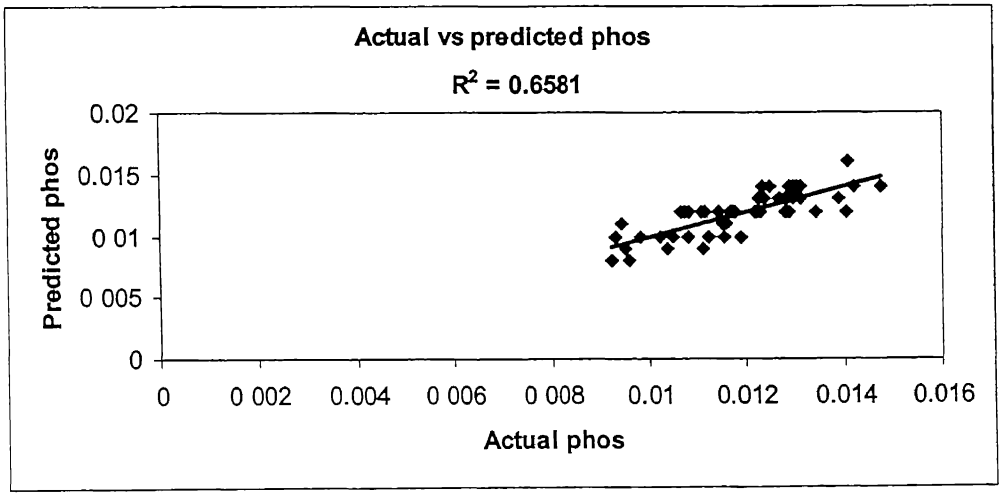

Fig 5.12 Comparison between actual and predicted phosphorous at the end of blow by modified Molecular theory model (Eq. 4.35)

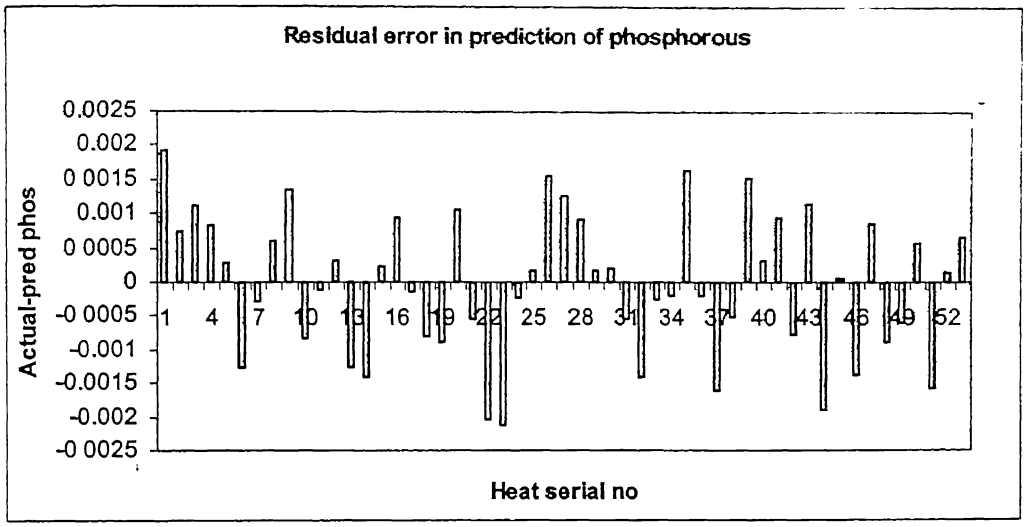

Fig- 5.13 Residual error plot for prediction of turndown phosphorous by modified Molecular theory model for case study-4 case-B (Eq. 5.6)

Chapter 6

Conclusions

(1) The models available in literature for prediction of phosphorus in steel are reviewed. Healy' model, Molecular slag model, Optical Basicity model and Quadratic Formalism model have been selected and tested for 3 different case studies with different hot metal and slag composition. It has been found that Molecular slag model gives the best results in all the cases.

(2) Prediction of turndown phosphorous is better, when either ore or raw dolomite is added during 2^{nd} part of the blow, but prediction is poorer if none of them is added during 2^{nd} part of the blow.

(3) Coefficient of turndown carbon is negative in low phosphorous hot metal and low MgO slag practice.

(4) Incorporation of C_2S as an additional parameter in the model improves the correlation coefficient for the prediction of turn down phosphorous.

(5) Solubility of phosphorous is much more in C_2S (4.5-6 %) than the wustite solid solution (0.3% max).

(6) Formation of dicalcium silicate is hindered by the presence of MgO and Al_2O_3 in slag.

(7) Size of dicalcium silicate grains as well as the dissolution of phosphorous in C_2S is decreases if slag contains more MgO and Al_2O_3.

Appendix-A

Calculation of activity of FeO by different methods

Method-1

Activity coefficient of FeO (γ_{FeO}) can be determined by regular solution method is as follows;

$$RT\ln\gamma_{FeO} = -31380\times X_{CaO}^2 - 41840\times X_{SiO_2}^2 + 60670\times X_{CaO}\times X_{SiO_2} - 8540 - 7.172\times T \quad .....(A.1)$$

Where, X_{CaO} and X_{SiO_2} are mole fraction of CaO and SiO_2 respectively.

Activity of FeO $(a_{FeO}) = \gamma_{FeO}\times X_{FeO}$ .....(A.2)

γ_{FeO} is activity coefficient of FeO which is calculated according to Eq. (A.1)

Method-2

Consider base is 100kg slag, which contains 50% CaO, 15% SiO2 7% MgO, 19 % FeO, 5% MnO, 2%Al_2O_3, 2% P_2O_5.

$$M_{CaO} = \frac{50}{56} kmoles$$

$$M_{FeO} = \frac{19}{72} kmoles$$

$$M_{MnO} = \frac{5}{71} kmoles$$

$$M_{MgO} = \frac{7}{40} kmoles$$

$$M_{SiO_2} = \frac{15}{60} kmoles$$

$$M_{Al_2O_3} = \frac{2}{102} kmoles$$

$$M_{P_2O_5} = \frac{2}{142} kmoles$$

The activity coefficient of FeO according to modified ionic theory model described in chapter 2 is as follows;

$$\log \gamma_{FeO} = -9\,405 \times N'_{O^{2-}} + 24.97 \times (N'_{O^{2-}})^2 + 2.018 \qquad \text{.....(A.3)}$$

The activity of FeO is defined as follows:

$$\begin{aligned} a_{FeO} &= a_{Fe^{2+}} \times a_{O^{2-}} \\ &= \gamma_{Fe^{2+}} \times N'_{Fe^{2+}} \times \gamma_{O^{2-}} \times N'_{O^{2-}} \\ &= \gamma_{FeO} \times N'_{Fe^{2+}} \times N'_{O^{2-}} \end{aligned} \qquad \text{.....(A.4)}$$

Calculation of $N'_{O^{2-}}$ (electrically equivalent ion fraction of oxygen ion):

A slag consisting of M_{CaO} moles of CaO, M_{FeO} moles of FeO, M_{SiO_2} moles of SiO2, M_{MnO} moles of MnO, M_{MgO} moles of MgO, $M_{Al_2O_3}$ moles of Al2O3 and $M_{P_2O_5}$ moles of P2O5 will dissociate into ions according to the scheme

$$\begin{aligned} &M_{CaO} + M_{FeO} + M_{MnO} + M_{MgO} + M_{SiO_2} + M_{Al_2O_3} + M_{P_2O_5} = \\ &M_{SiO_4^{4-}} + 2 \times M_{PO_4^{3-}} + 3 \times M_{AlO_3^{3-}} + [(M_{CaO} + M_{FeO} + M_{MnO} + M_{MgO}) \\ &-(2 \times M_{SiO_2} + 3 \times M_{Al_2O_3} + 3 \times M_{P_2O_5})]O^{2-} + M_{Ca^{2+}} + M_{Fe^{2+}} + M_{Mn^{2+}} + M_{Mg^{2+}} \end{aligned} \qquad \text{.....(A.5)}$$

The electrically equivalent ion fraction of O^{2-} is given by;

$$N'_{O^{2-}} = \frac{2\times[(M_{CaO}+M_{FeO}+M_{MnO}+M_{MgO})-(2\times M_{SiO_2}+3\times M_{Al_2O_3}+3\times M_{P_2O_5})]}{4\times M_{SiO_4^{4-}}+6\times M_{PO_4^{3-}}+6\times M_{AlO_3^{3-}}+2[(M_{CaO}+M_{FeO}+M_{MnO}+M_{MgO})-(2\times M_{SiO_2}+3\times M_{Al_2O_3}+3\times M_{P_2O_5})]O^{2-}}$$

$$= \frac{2\times\left[\left(\frac{50}{56}+\frac{19}{72}+\frac{5}{71}+\frac{7}{40}\right)-\left(2\times\frac{15}{60}+3\times\frac{2}{102}+3\times\frac{2}{142}\right)\right]}{4\times\frac{15}{60}+6\times\frac{2}{142}+6\times\frac{2}{102}+2\left[\left(\frac{50}{56}+\frac{19}{72}+\frac{5}{71}+\frac{7}{40}\right)-\left(2\times\frac{15}{60}+3\times\frac{2}{102}+3\times\frac{2}{142}\right)\right]} \quad \text{.....(A.6)}$$

The multiplication by 2 in the numerator refers to the negative charge of 2 on O^{2-} ions.

$(M_{CaO}+M_{FeO}+M_{MnO}+M_{MgO})$=Total oxygen ions produced by dissociation of all the basic oxides.

$(2\times M_{SiO_2}+3\times M_{Al_2O_3}+3\times M_{P_2O_5})$=total oxygen ions consumed by acid oxides.

$4\times M_{SiO_4^{4-}}+6\times M_{PO_4^{3-}}+6\times M_{AlO_3^{3-}}+2[(M_{CaO}+M_{FeO}+M_{MnO}+M_{MgO})-(2\times M_{SiO_2}+3\times M_{Al_2O_3}+3\times M_{P_2O_5})]O^{2-}$
is total negative charge available

Combining Eq. A.3, A.4 and A.6 activity of FeO is calculated

Appendix-B

Calculation of percentage dicalcium silicate for an over all slag composition from the ternary phase diagram of CaO-FeO-SiO_2.

We assume the slag is quasi ternary i e. it essentially contains CaO, FeO and SiO_2 or [(%CaO) + (%SiO2) + (%FeO)] =100.

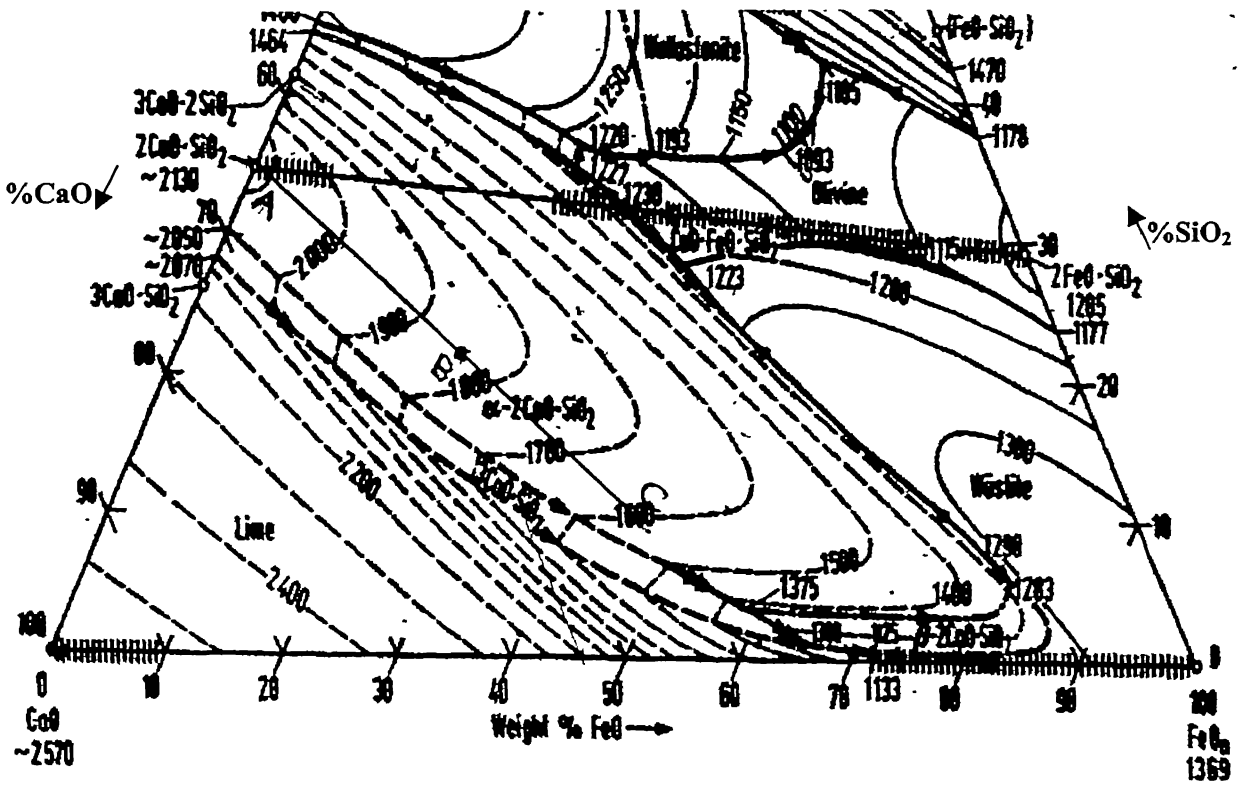

Fig-A 1 Ternary phase diagram of CaO-FeO-SiO_2

Point B in the above diagram is corresponding to a slag composition of 55 percent (CaO), 23 percent (SiO_2) and 22 percent (FeO). Point (A) in the diagram is for 100 percent dicalcium silicate. First we connect point A and point B and extend the line AB to the liquidus at 1600^{0}C. It intersects the liquidus at point C.

Now according to liver rule percent solid is $= \frac{BC}{AC} \times 100\% = \frac{28}{61} \times 100\% = 45.9\%$

Percent dicalcium silicate at 1600^0C for the slag composition is 45.9%.

Appendix-C

Calculation procedure of liquid slag composition

Consider that the slag consist of 50% CaO, 15% SiO2 7% MgO, 19 % FeO, 5% MnO, 2%Al_2O_3, 2% P_2O_5 and turndown temperature is 1705^{0}C and total slag mass is 100kg. Calculation of percentage dicalcium silicate (2CaO.SiO2) has been described in appendix-1.

Considering slag is quasi-ternary i.e. the slag contains CaO, FeO and SiO2 only. The percentage dicalcium silicate can be calculated according to appendix-1. Percentage C_2S is 21.21 liquid fraction 75.92 percent CaO in solid slag 2.87.

So,
Total Mass of CaO= 50kg

Total Mass of SiO2=15kg

Total Mass of FeO=19kg

Total Mass of MgO=7kg

Total Mass of MnO=5kg

Total Mass of Al_2O_3=2kg

Total Mass of P_2O_5=2kg

Over all Slag basicity $\frac{(\%CaO)}{(\%SiO_2)} = \frac{50}{15} = 3.33$

Mass if quasi-ternary slag= (50+15+19) kg=84kg

Total mass of (MgO+ MnO+ Al_2O_3+ P_2O_5) = (7+5+2+2) kg=16kg, this is a part of liquid slag.

So total mass of liquid slag= Mass of liquid fraction of quasi-ternary slag+ Total mass of (MgO+MnO+ Al_2O_3+ P_2O_5)

$$mass\ of\ liquid\ slag = \left(\frac{75.92 \times 84}{100} + 16\right) kg = 79.77\, kg \qquad \text{..... ....} (C.1)$$

$$mass\ of\ dicalcium\ silicate = \frac{21.21\times 84}{100} kg = 17.81 kg \quad \text{.....(C.2)}$$

$$mass\ of\ solid\ CaO = \frac{2.87\times 84}{100} kg = 2.41 kg \quad \text{.....(C.3)}$$

$$\text{Mass of CaO in dicalcium silicate} = \frac{\text{Mass of dicalcium silicate}\times 112}{172} kg$$

$$= \frac{17.81\times 112}{172} kg = 11.6 kg \quad \text{.....(C.4)}$$

So,

Mass of CaO in liquid slag= (Total mass of CaO in overall slag-Mass of CaO in dicalcium silicate-mass of solid CaO).

Mass of CaO in liquid slag= (50-11.6-2.4) =36

$$\text{Mass of } SiO_2 \text{ in dicalcium silicate} = \frac{17.81\times 60}{172} kg = 6.21 kg \quad \text{.....(C.5)}$$

Mass of SiO_2 in liquid slag= (Total Mass of SiO_2- Mass of SiO_2 in dicalcium silicate).
= (15-6.2) kg =8.8kg

So new liquid slag composition will be as follows,

$$Percent\ \text{CaO in liquid slag} = \frac{mass\ of\ CaO\ in\ liquid\ slag\times 100}{mass\ of\ liquid\ slag}$$

$$= \frac{36\times 100}{79.77} = 45\% \text{.....(C.6)}$$

$$Percent\ SiO_2\ in\ liquid\ slag = \frac{mass\ of\ SiO_2\ in\ liquid\ slag\times 100}{mass\ of\ liquid\ slag}$$

$$= \frac{8.8\times 100}{79.77} = 11\% \text{ ....(C.7)}$$

$$Percent\ of\ FeO\ in\ liquid\ slag = \frac{mass\ of\ FeO\times 100}{mass\ of\ liquid\ slag}$$

$$= \frac{19\times 100}{79.77} = 23.8\% \quad \text{.....(C.8)}$$

$$Percent\ of\ MgO\ in\ liquid\ slag = \frac{mass\ of\ MgO \times 100}{mass\ of\ liquid\ slag}$$

$$= \frac{7 \times 100}{79.77} = 8.8\% \quad .....(B.9)$$

$$Percent\ of\ MnO\ in\ liquid\ slag = \frac{mass\ of\ MnO \times 100}{mass\ of\ liquid\ slag}$$

$$= \frac{5 \times 100}{79.77} = 6.27\% .....(B.10)$$

$$Percent\ of\ Al_2O_3\ in\ liquid\ slag = \frac{mass\ of\ Al_2O_3 \times 100}{mass\ of\ liquid\ slag}$$

$$= \frac{2 \times 100}{79.77} = 2.5\% .....(B.11)$$

$$liquid\ slag\ basicity = \frac{percent\ CaO\ in liquid\ slag}{percent\ SiO_2\ in liqui dslag}$$

$$= \frac{45}{11} = 4.09 .....(B.12)$$

Therefore liquid slag basicity is higher than the over all slag basicity.

References

1. K. Balajiva, A.G. Quarell, and P. Vajragupta, "A laboratory Investigation of the Phosphorous reactions in the Basic Steelmaking Process" Journal of Iron and Steel institute, Vol.153, 1946, pp. 115.

2. E.T.Turkdogan, "Fundamentals of Steelmaking", The Inst. of Materials, London, 1996.

3. G.H.Healy, "A NEW LOOK AT PHOSPHOROUS DISTRIBUTION", Journal of iron and steel institute Vol.177, 1970, pp664-668.

4. G. Thornton and D.Anderson, "Low Phosphorous Basic Oxygen Steelmaking Practices in British Steelmaking" Ironmaking and Steelmaking, Vol.21 , No.3, 1994, pp. 247-251.

5. J.A. Duffy., and M.D. Ingram, "Establishment of an optical scale for Lewis basicity in inorganic oxyacids, molten salts, and glasses ", J. Am. Ch. Soc., 1971-73, pp.6448-6455.

6. R.W. Young, J.A. Duffy, G.J. Hassall, and Z.Xu, "Use of Optical Basicity Concept For determining Phosphorous and Slag Metal Partition.", Iron Making and Steel Making, Vol.19, No.3, 1992, pp.213.

7. H. Suito and R. Inoue, "Phosphorous Distribution Between MgO Saturated CaO-Fe_tO –SiO_2-P_2O_5 slag" Trans. ISIJ., Vol. 24, 1984, pp. 40-46.

8. J.F. Eliott, D.C. Lynch and T.B. Barun, "A criticism of the Flood-Grjotheim Ionic Treatment of Slag-Metal Equilibra", Met. Trans. B, Vol. 6B, 1975, pp. 495-502.

9. S. BAN-YA, "Mathematical Expression of Phosphorous Distribution in Steelmaking Process by Quadratic Formalism", ISIJ International, Vol.33, No.1, 1993, pp. 140-147.